Marine Pollution Bulletin 180 (2022) 113776

Contents lists available at ScienceDirect

Marine Pollution Bulletin

journal homepage: www.elsevier.com/locate/marpolbul

Baseline

Spatiotemporal distribution characteristics of yessotoxins and pectenotoxins in phytoplankton and shellfish collected from the southern coast of South Korea

Mungi Kim [a], Seongjin Hong [a,*], Young Kyun Lim [b,c], Jihyun Cha [a], Jiyun Gwak [a], Youngnam Kim [a], Seong-Ah An [a], Hee-Seok Lee [d], Seung Ho Baek [b,c,*]

[a] Department of Ocean Environmental Sciences, Chungnam National University, Daejeon 34134, Republic of Korea
[b] Risk Assessment Research Center, Korea Institute of Ocean Science and Technology, Geoje 53201, Republic of Korea
[c] Department of Ocean Science, University of Science and Technology, Daejeon 34113, Republic of Korea
[d] Department of Food Science and Technology, Chung-Ang University, Anseong 17546, Republic of Korea

ARTICLE INFO

Keywords:
Lipophilic marine biotoxins
Shellfish
Causative microalgae
LC-MS/MS
Risk assessment

ABSTRACT

The distribution characteristics of lipophilic marine biotoxins (LMTs), such as yessotoxins (YTXs) and pectenotoxins (PTXs) in phytoplankton, mussels, and commercial seafood were determined for the southern coast of South Korea. *Gonyaulax spinifera* and *Dinophysis acuminata*, which are the causative microalgae of YTXs and PTXs, were recorded during summer. Homo-YTX and PTX-2 were predominantly detected in phytoplankton (max: 5.7 μg g^{-1} ww), whereas only YTXs were detected in mussels (max: 1.1 μg g^{-1} ww). LMT concentrations in mussels were positively correlated with those in phytoplankton. However, there was a 1-month time gap in maximum LMT concentrations between mussels and phytoplankton. Homo-YTX was detected in commercial seafood, including red scallop and comb pen shell. However, homo-YTX concentrations in shellfish were below the recommended value of the European Food Safety Authority (3.75 mg YTX equivalents kg^{-1}); thus, the consumption of this seafood was not considered to be a significant risk for human health.

Harmful algal blooms (HABs), which can adversely affect marine ecosystems, occur globally, and are increasing in frequency, associated with climate change (Gobler et al., 2017), eutrophication, and expansion of coastal aquaculture (Hallegraeff et al., 2021). Some harmful microalgae naturally produce marine biotoxins that accumulate in filter-feeding organisms, such as bivalves (Liu et al., 2019; Reguera et al., 2012). Marine biotoxins can be transformed to produce many toxic metabolites in bivalves (Yasumoto, 2005), which threaten human health when contaminated shellfish are consumed.

Marine biotoxins are generally classified into hydrophilic and lipophilic biotoxins according to their chemical properties, such as polarity (Chen et al., 2017). More than 200 marine biotoxins have been identified so far (Gerssen et al., 2011), and more than 90% of marine biotoxins belong to lipophilic marine biotoxins (LMTs) (Wang et al., 2015). Representative LMTs include okadaic acid (OA), dinophysistoxins (DTXs), yessotoxins (YTXs), pectenotoxins (PTXs), brevetoxins (BTXs), and azaspiracids (AZAs). Hydrophilic marine biotoxins include domoic acid (DA) and saxitoxin (STX). LMT poisoning of shellfish has been reported in the coastal areas of various countries, including China, Italy, and Norway (Draisci et al., 1999; Liu et al., 2019; MacKenzie et al., 2002; Ramstad et al., 2001). Cases of LMTs contamination in shellfish are continuously increasing, with areas of biotoxin contamination gradually expanding (Hallegraeff et al., 2021). Consequently, the risk of seafood to human health following consumption is of great concern.

Along the southern coast of Korea, HABs have been reported over the last four decades (Baek et al., 2020; Kim et al., 2019). HABs are caused by *Prorocentrum* spp., *Gyrodinium* spp., *Gymnodinium* spp., *Heterocapsa* spp., *Karenia* spp., *Pseudo-nitzschia* spp., *Thalassionema* spp., and *Cryptomonas* spp. (Baek et al., 2020; Kim et al., 2019). In the South Sea, cultured shellfish frequently die due to high seawater temperature and hypoxic conditions. The growth of shellfish is inhibited by changes to the species composition of phytoplankton, resulting in the number of individuals declining (Lee et al., 2019). The South Sea accounts for 95% of shellfish culture production in South Korea, including scallops, oysters, cockles, and mussels (Lee et al., 2019). Monitoring is regularly performed for certain shellfish toxins, including paralytic shellfish

* Corresponding authors.
E-mail addresses: hongseongjin@cnu.ac.kr (S. Hong), baeksh@kiost.ac.kr (S.H. Baek).

https://doi.org/10.1016/j.marpolbul.2022.113776
Received 31 March 2022; Received in revised form 17 May 2022; Accepted 18 May 2022

poisoning (PSP), diarrhetic shellfish poisoning (DSP), and amnesic shellfish poisoning (ASP) (MFDS, 2009). There have been investigations on the contamination status of unmanaged biotoxins in domestic seafood, but cases of seafood contamination from these toxins have not yet been reported on the southern coast of Korea.

YTXs and PTXs are well-known LMTs. The causative microalgae of YTXs are *Gonyaulax spinifera*, *Protoceratium reticulatum*, and *Lingulodinium polyedrum* (Paz et al., 2007; Satake et al., 1999; Suzuki et al., 2007). In comparison, PTXs are mainly produced by *Dinophysis fortii*, *D. acuminata*, and *D. caudata* (Li et al., 2017; Pizarro et al., 2008; Reguera et al., 2014). YTXs were previously included in the DSP group (Paz et al., 2008); however, recent studies reported that YTXs do not cause diarrhea, but do affect the myocardium (Ferreiro et al., 2016; Paz et al., 2008). PTXs are also hepatotoxins rather than causing diarrhea (Terao et al., 1993). The European Food Safety Authority (EFSA) recommended setting minimum thresholds for YTXs and PTXs, to prevent accidents caused by the ingestion of shellfish contaminated with them (EFSA, 2008, 2009); however, regulations on these toxins have not yet been established in South Korea. At present, as the sea surface temperature increases due to global climate change, the distribution range of subtropical harmful microalgae is extending (Gobler et al., 2017). Consequently, exotic microalgae might appear in Korean coastal waters, and unmanaged shellfish toxins could occur. However, to date, LMTs (such as YTXs and PTXs) are rarely monitored in Korea. As a result, their distribution characteristics are largely unknown.

In the present study, we investigated the spatiotemporal distributions of YTXs and PTXs along the southern coast of South Korea. The specific objectives were to: i) identify the causative microalgae from summer to winter, ii) determine concentrations of YTXs and PTXs in phytoplankton and field mussels, iii) investigate YTXs and PTXs contamination of various commercial shellfish, and iv) assess the potential risk of YTXs and PTXs to human health through seafood consumption.

The field investigation and sampling were conducted monthly at 13 sites (Group 1: S1–S7; Group 2: S8–S13) along the southern coast of Korea from June to December 2020 (Fig. 1). Water quality parameters were measured in situ using a multi-sensor (YSI 6600v2, YSI Inc., Yellow Springs, OH), and included water temperature (WT), salinity, pH, and dissolved oxygen (DO). Dissolved inorganic nutrients (NO_2^-, NO_3^-, NH_4^+, PO_4^{3-}, and SiO_2) were analyzed using an automatic nutrient analyzer (LACHAT Quikchem 8000, Hach Company, Loveland, CO). The concentration was quantified using reference materials for nutrients in seawater (KANSO Technos Co., Osaka, Japan). Chlorophyll-a (Chl.a) was extracted with 90% acetone in the dark for 24 h, and was measured using a Turner-designed fluorometer (Turner BioSystems, Sunnyvale, CA) (Lim et al., 2019).

To analyze the density and species composition of phytoplankton, 500 mL of surface seawater was collected and immediately fixed with Lugol solution (final concentration 3%). The fixed sample in the laboratory was concentrated to 50 mL, transferred to the Sedgewick-Rafter Chamber, and allowed to settle for 10 min. Phytoplankton species were identified using a light microscope. Morphologically distinct species were identified at the species level, and indistinguishable species were identified at the genus level.

Phytoplankton samples (20–200 μm suspended particulate matter (SPM), $n = 89$) were collected using a 20 μm mesh net. Zooplankton and large suspended solids were removed using a 200 μm mesh net. Then, the concentrated phytoplankton (about 150 mL) was filtered with nylon net filters (20 μm, 47 mm, Millipore, Merck, Darmstadt, Germany), and the samples were stored at −20 °C until analysis. To analyze YTXs and PTXs in phytoplankton, the frozen filter was thawed at room temperature, cut with scissors, and placed in a 15 mL conical tube. The sample was extracted with 3 mL methanol, and was vortex-mixed for 1 min (Liu et al., 2017). After sonication for 5 min, the supernatant was collected by centrifugation at 3500 rpm for 10 min. The same process was repeated two more times, and the extracts were combined (final volume 10 mL). The extract was filtered through a 0.22 μm syringe filter before instrumental analysis.

Mussels ($n = 75$) were collected monthly from the same field sites (S1–S13) as the phytoplankton. More than 20 mussels were collected

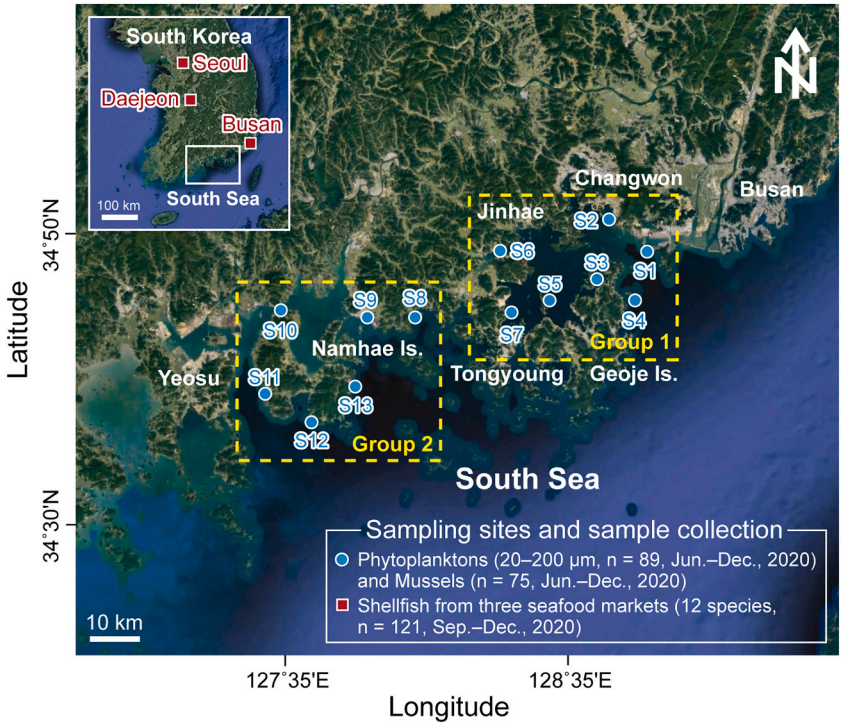

Fig. 1. Sampling sites of phytoplankton, mussels, and shellfish. Phytoplankton (20–200 μm SPM) and mussels were collected from Sites S1–S13 along the southern coast of South Korea (June to December 2020). Shellfish samples were collected from three seafood markets located in Seoul, Daejeon, and Busan (September to December 2020).

from each site at each sampling event. The mussels were transferred to the laboratory in a cool box, and were stored at −20 °C until analysis. Domestic seafood samples ($n = 121$) were collected monthly from three seafood markets located in Seoul, Daejeon, and Busan from September to December 2020 (Fig. 1). Twelve species of commercial shellfish were collected; namely ark shell, red shell, mussel, corb shell, surf clam, hard clam, purplish clam, marsh clam, comb pen shell, red scallop, manila clam, and oyster. The scientific names and sample information of commercial shellfish are present in Table S1 of the Supplementary Materials. The collected shellfish were transferred to the laboratory, and were stored at −20 °C until analysis.

After removing the shell of the bivalves, the soft tissue was collected and homogenized. More than 20 individuals per sample were pooled. Two grams of the homogenized sample were extracted with 9 mL of 100% methanol and vortex-mixed for 1 min (Orellana et al., 2014). The extract was sonicated in ice water for 10 min, and was then centrifuged at 3500 rpm for 10 min to collect the supernatant. The same process was repeated twice, and the final volume was made up to 20 mL. Solid-phase extraction (SPE) cartridge (Strata-X, 30 mg, 3 mL, Phenomenex, Torrance, CA) was used to remove interfering substances. The SPE cartridge was activated with 3 mL methanol and 3 mL deionized water. After diluting the methanol content of the extract to 20% or less, it was loaded into the cartridge. After loading the sample, the cartridge was washed with 3 mL of 15% methanol and dried under vacuum for 3 min. YTXs and PTXs were eluted with 3 mL methanol containing 1% ammonium hydroxide, and were concentrated to 1 mL under N_2 gas.

Authentic standards for YTX, homo-YTX, PTX-2, and PTX-11 were obtained from the National Research Council of Canada (Ottawa, ON, Canada) and Sigma-Aldrich (St. Louis, MO). LMTs were analyzed using an Agilent 1290 Infinity II LC system (Agilent Technologies, Santa Clara, CA) coupled with an Agilent 6470 triple quadrupole mass spectrometer MS/MS system (Agilent Technologies). LMTs were separated using a Waters X-Bridge C18 column (3.0 mm × 150 mm, 5.0 μm). The mobile phase consisted of (A) 0.05% ammonium hydroxide in water and (B) 0.05% ammonium hydroxide in 90% acetonitrile in water. Target LMTs were analyzed using multiple reaction monitoring (MRM) mode. YTXs and PTXs were detected in negative and positive modes, respectively. Details on MRM transitions and mobile phase gradient conditions are provided in Tables S2 and S3.

A matrix-spiked calibration curve, in the range of 1.0 to 50 ng mL^{-1} (six levels), was used to quantify LMTs ($R^2 > 0.996$). Limit of detection (LOD) and limit of quantification (LOQ) were calculated by analyzing a mussel spiked with standard materials (1 ng, $n = 7$). LOD and LOQ were calculated by multiplying the standard deviation of the spiked mussel extract response by 3.143 and 10, respectively. LOD and LOQ ranged from 1.6 to 3.3 ng g^{-1} wet weight (ww) and 5.1 to 10.5 ng g^{-1} ww, respectively. The recovery rate of each LMT was analyzed for mussels were spiked with standard materials (25 ng), following the procedure described above ($n = 4$). Recoveries of the spike test ranged from 91 to 98% (details in Table S4).

For statistical analysis, IBM SPSS Statistics 26 (Armonk, NY) and R software (Version. 3.6.3) were used. Shapiro-Wilk's normality test was performed to verify the normality of the data, and the data obtained from the present study did not satisfy a normal distribution. The Mann-Whitney test was conducted to confirm the difference in LMT concentrations between Group 1 and Group 2. Spearman's rank correlation and principal component analysis (PCA) were carried out to evaluate significant relationship between LMT concentrations, water quality parameters, and the abundance of causative microalgae. All significance levels were set at 0.05 (p-value). Values with LMT concentrations below LOD were analyzed using LOD/2. Redundancy analysis (RDA) was performed using CANOCO version 4.5 to investigate the relationship between environmental variables and phytoplankton dynamics. Environmental variables (e.g., DO, pH, WT, salinity, and nutrients) were used in the analysis. Data used for RDA were square root converted and analyzed.

Exposure of YTXs and PTXs was assessed based on the consumption of commercial shellfish. The consumption data of shellfish were estimated from the 7th period of the Korean National Health and Nutrition Examination Survey (KNHANES, 2016–2018) conducted by the Korean Disease Control and Prevention Agency (KCDA, 2020). Consumption data of bivalves were assessed using a 24-h dietary recall questionnaire. Daily food intake was analyzed based on bivalve group. The consumption of red scallops and comb pen shells was calculated. For the exposure assessment of YTX and homo-YTX by intake of bivalves with acute reference dose (ARfD) values, we established four consumption scenarios with the highest detected concentration according to FAO/WHO guidance (FAO/WHO, 2011) and the EFSA report (EFSA, 2008), as follows (Eqs. (1)–(4)):

$$\text{Scenario 1} : \text{Highest detection concentration} \times \text{mean consumption} \quad (1)$$

$$\text{Scenario 2} : \text{Highest detection concentration} \times \text{high consumption I} \quad (2)$$

$$\text{Scenario 3} : \text{Highest detection concentration} \times \text{high consumption II} \quad (3)$$

$$\text{Scenario 4} : \text{Highest detection concentration} \times \text{high consumption III} \quad (4)$$

where mean consumption indicates food consumption by all participants. High consumption I, II, and III indicate food consumption by only consumers, 95th level of food consumption by all participants, and 97.5th level of food consumption by all participants, respectively.

The hazard quotient (HQ%) and hazard index (HI%) were calculated to estimate the exposure level by comparing the estimated daily intake (EDI) with the ARfD value. Based on a previous report (EFSA, 2008), 25 μg YTX equivalent (EQ) kg^{-1} body weight was applied as the ARfD for YTX and homo-YTX, because the toxic equivalence factor of YTX and homo-YTX is 1. By considering the Korean mean body weight (60 kg) suggested in the KNHANES, the health-based guidance value (HbGV) of 1500 μg YTX EQs/person/day was utilized. As the sum of HQs for each contaminated bivalve, the HI% for each compound was calculated using Eq. (5) in accordance with the method for mixture-risk assessment of chemical risk factors (Juan-Borrás et al., 2016).

$$HI\% = \left(\sum\nolimits_{n=1}^{i} HQ_n\%\right) \left[HQ\% = \left(\frac{EDI}{HbGV}\right) \times 100\right] \quad (5)$$

The water quality parameters of the southern Korean coast from June to December are shown in Table S5. Notable parameters of seawater quality included variation in salinity and nutrients. In August, salinity was less than 30 psu at all sites. The concentrations of nutrients showed large spatial and temporal variation, with relatively high concentrations being observed in July and August. The average precipitation one week before the sampling campaign was observed to be 30 mm per day, indicating that rainwater had an influence. In addition, freshwater discharge from the Yangtze River reached a maximum of 82,000 tons s^{-1} in July 2020. The South Sea is affected by the Tsushima Warm Current during summer and fall, and is affected by freshwater from the Yangtze River after the summer monsoon (Chang, 2003; Isobe, 1999). In addition, nutrient concentrations in seawater are affected by the formation of stratification and inflow of runoff after heavy rainfall (Baek et al., 2015; Lee et al., 2018). These factors seem to be related to variation in water quality. This phenomenon occurs annually in the South Sea of Korea (Lim et al., 2019).

The species composition and density of phytoplankton, as well as LMT concentrations in organisms, were interpreted by dividing the sampling sites into the eastern region near Jinhae Bay (Group 1: S1–S7) and the western region near Namhae Is (Group 2: S8–S13) (Fig. 1). At all sites, phytoplankton included Bacillariophyceae (57 ± 16%), Cryptophyceae (28 ± 21%), Dinophyceae (13 ± 5%), Raphidophyceae (0.49 ± 1.2%), and Dictyochophyceae (0.26 ± 0.34%), supporting previous studies conducted in the South Sea (Baek et al., 2019; Lim et al., 2019, 2021). In general, *Skeletonema* spp. and *Pseudo-nitzschia* spp. occupied

cold seawater with rich nutrient conditions, whereas dinoflagellates occupied warmer water (Fig. S1). The succession from diatoms to dinoflagellates was previously reported to occur in the South Sea during summer (Lim et al., 2019). In the current study, the succession from diatoms to dinoflagellates also occurred during summer; however, the timing of succession differed between Group 1 and Group 2. For example, the relative contribution of Dinophyceae in Group 1 increased from 10% in June to 29% in July. In contrast, in Group 2, its contribution increased from 8.5% in July to 28% in August. In the previous study, phytoplankton communities between Group 1 and Group 2 were statistically distinguished (Baek et al., 2020). The succession of diatoms and dinoflagellates was closely related to the vertical structure of nutrients in the water column (Lim et al., 2019; Baek et al., 2019). In this study, as other environmental factors were similar between the two groups, nutrients were considered to be the major factor controlling the succession of diatoms and dinoflagellates.

The density of phytoplankton in Group 1 and Group 2 ranged from 52 to 5230 cells mL^{-1} and 48 to 2670 cells mL^{-1}, respectively (Table S6). There was no significant difference in the density of phytoplankton between the two groups ($p > 0.05$). The maximum density of both groups occurred during summer. After September, the average density decreased to below 1000 cells mL^{-1} in both groups. This result was similar to a previous study (Baek et al., 2019). In the South Sea, the species composition and density of phytoplankton showed seasonal variability, and the timing of succession appeared to differ with region. To identify major environmental factors controlling the composition of phytoplankton, statistical analysis was performed on the top 15 species identified in this study. RDA showed that diatoms and dinoflagellates were positively correlated with nutrients. In contrast, salinity was negatively correlated with nutrients (Fig. S2). This result might be attributed to the inflow of nutrient-rich freshwater in summer causing salinity to decrease and phytoplankton levels to increase. Chl.a and water temperature were strongly correlated with certain diatoms, including *Chaetoceros* spp. and *Pseudo-nitzschia* spp., which might be associated with high biomass during summer. Baek et al. (2020) also previously showed a strong positive relationship of these two species with Chl.a, which is a biomass indicator of phytoplankton in the South Sea.

Gonyaulax spinifera and *D. acuminata* are known causative microalgae of YTXs and PTXs, respectively, and were found on the southern coast of Korea (Fig. 2 and Table S7). The presence of YTX-producing microalgae has not been previously reported in the coastal waters of Korea; however, it has been confirmed that they exist in the form of cysts in sediments of the South Sea (Yoon and Park, 2017). *Gonyaulax spinifera* exhibited no significant difference in density between the two groups ($p > 0.05$). Its density peaked during June and August in Group 1 and Group 2, respectively. The density of *G. spinifera* was relatively higher in summer, and tended to decline after August. The density of *D. acuminata* was lower compared to *G. spinifera*; however, its density was also relatively higher during summer. In contrast, Kim et al. (2010) recorded much lower densities of *D. acuminata* in Group 1 (1 cell mL^{-1}). Overall, relatively high densities of LMT-producing microalgae were documented in the southern sea during summer in our study, which is a concern for the poisoning of shellfish. In addition, although domoic acid could not be analyzed in this study, the causative algae, *Pseudo-nitzschia* spp., was present at high densities (>10,000 cells L^{-1}); thus, further investigation on domoic acid poisoning in shellfish is needed (Table S7).

Homo-YTX, PTX-2, and PTX-11 were detected in phytoplankton (20–200 μm SPM) along the southern coast of Korea during the sampling period. The concentrations of these toxins varied across sites, indicating heterogeneous distributions (Fig. 3a and Table S8). The concentrations of homo-YTX, PTX-2, and PTX-11 in Group 1 were <LOD–0.48 μg g^{-1} ww, <LOD–0.43 μg g^{-1} ww, and <LOD–0.18 μg g^{-1} ww, respectively. In Group 2, the concentrations of homo-YTX and PTX-2 were <LOD–5.7 μg g^{-1} ww and <LOD–0.058 μg g^{-1} ww, respectively. There was no significant difference in LMT concentrations between the two groups, except for June ($p > 0.05$), and PTX-11 was only detected in Group 1. This result might be attributed to *D. acuminata*, the causative microalgae of PTXs, occurring at relatively high densities in Group 1. To date, the detection of homo-YTX and PTX-11 in phytoplankton along the southern coast has not been reported (this study provides the first report). However, small concentrations of PTX-2 were detected in the region of Group 1 by Kim et al. (2010). In both groups, relatively high concentrations of homo-YTX were recorded in summer (June–August) compared to fall and winter, with maximum concentrations occurring during June. LMT concentrations declined after August, and were not detected at most sites of Groups 1 and 2 from September to December. These results were similar to that recorded by Liu et al. (2021), in which relatively high concentrations of homo-YTX were detected in phytoplankton in southern China during summer.

In mussels collected from field sites, LMTs were only detected in YTX and homo-YTX, whereas PTXs were not detected in any samples (Fig. 3b and Table S9). In Group 1, the concentrations of YTX and homo-YTX were <LOD–0.041 μg g^{-1} ww and <LOD–0.77 μg g^{-1} ww, respectively. In Group 2, the concentrations of YTX and homo-YTX were <LOD–0.083 μg g^{-1} ww and <LOD–1.1 μg g^{-1} ww, respectively. Similar to LMT concentrations in phytoplankton, LMT concentrations in mussels were higher in Group 2 compared to Group 1. However, there was no

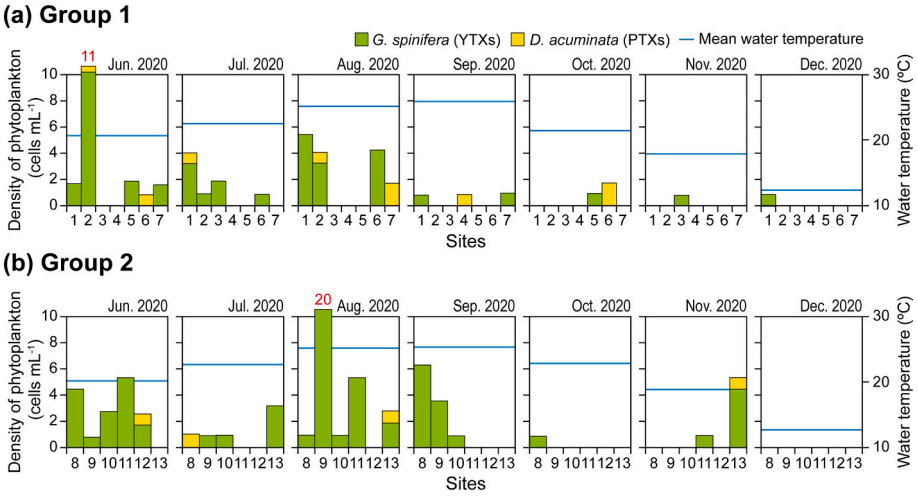

Fig. 2. Density of causative microalgae of YTXs and PTXs in (a) Group 1 and (b) Group 2 on the southern coast of South Korea from June to December 2020. Blue lines represent mean water temperature. (For interpretation of the references to color in this figure legend, the reader is referred to the web version of this article.)

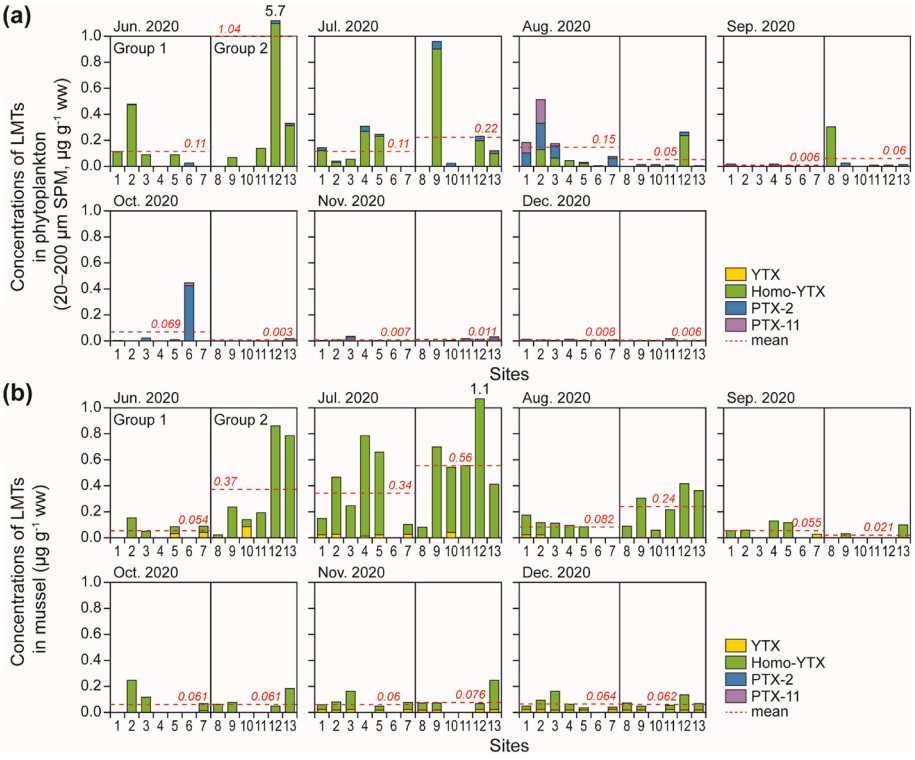

Fig. 3. Concentrations of YTXs and PTXs in (a) phytoplankton (20–200 μm SPM) and (b) mussels on the southern coast of South Korea from June to December 2020.

significant difference between the two groups ($p > 0.05$). LMT concentrations in mussels collected in the present study were higher compared to a previous study conducted in the South Sea (Kim et al., 2010). Only YTX and homo-YTX were detected in mussels, contrasting with LMT concentrations in phytoplankton, which might be due to mussels having a different biological half-life for LMTs. The half-life of PTXs in mussels was reported to be 2.9 d, which was relatively short compared to those of YTXs (range: 20 to 24 d) (Aasen et al., 2005; Nielsen et al., 2016). Although PTXs existed in phytoplankton, they were not detected in mussels because they were easily metabolized and excreted in mussels.

Similar to LMT concentrations in phytoplankton (20–200 μm SPM), those in mussels had a seasonal trend, with relatively higher

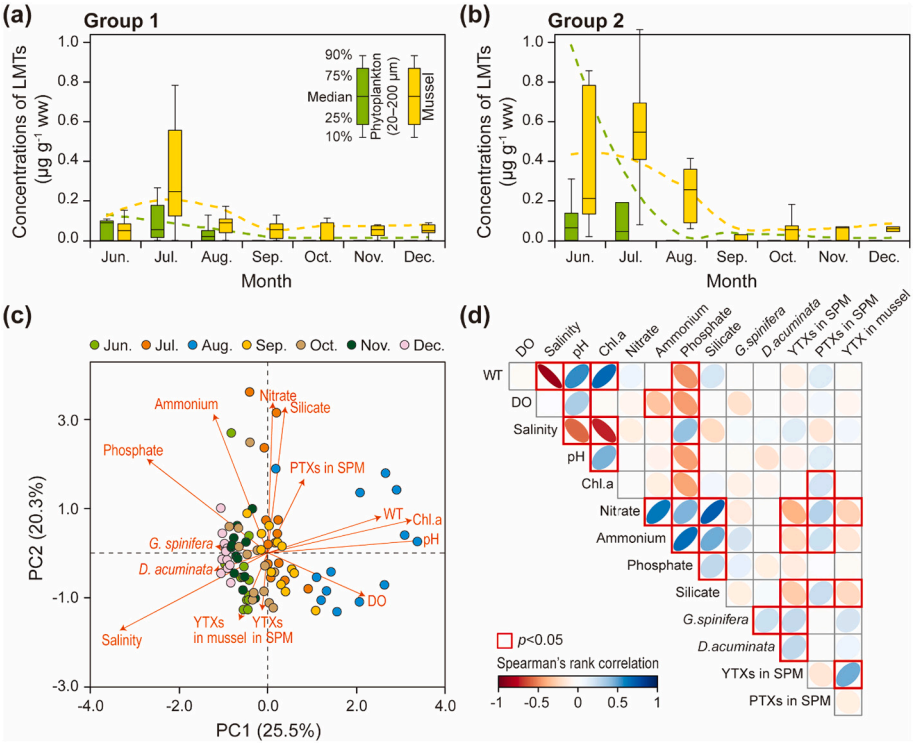

Fig. 4. Boxplot showing the concentrations of LMTs in phytoplankton (20–200 μm SPM) and mussels in (a) Group 1 and (b) Group 2 on the southern coast of South Korea from June to December 2020. Dotted lines are the fitted lines of the box plot. Fitted lines were created using the ggplot2 package in R software. (c) Results of the principal component analysis (PCA) based on environmental parameters, density of causative microalgae, and LMT concentrations. (d) Spearman's rank correlation between environmental parameters and LMT concentrations in organisms.

concentrations in summer (June–August), which declined after August. This result was comparable to that obtained by Kim et al. (2010). This phenomenon might be explained by seasonal variation in the presence of causative microalgae. For instance, *G. spinifera*, the microalgae causing YTXs, occurred at higher densities in summer, and then decreased, with very low densities (<1 cell mL^{-1}) after September. Compared to LMT concentrations in phytoplankton, those in mussels peaked later (Fig. 4a and b). For instance, LMT concentrations in phytoplankton and mussels peaked in June and July, respectively, at site S12, showing a 1-month difference. Li et al. (2017) reported that the densities of causative microalgae, *Dinophysis* spp. and *Phalacroma rotundatum*, peaked during summer, with LMT accumulation in shellfish being detected 1–2 weeks later (Li et al., 2017). Thus, LMTs, such as YTXs, appear to accumulate for longer in shellfish compared to phytoplankton, with the biological half-life of biotoxins playing a key role.

The relationship between environmental factors and LMT concentrations in phytoplankton (20–200 μm SPM) and mussels was analyzed statistically. In both groups, environmental factors showed no significant relationship with LMT concentrations in organisms (Figs. 4c and d, S3, $p > 0.05$). LMT concentrations in phytoplankton were significantly correlated to the densities of causative microalgae, not environmental factors. Homo-YTX concentrations in phytoplankton were significantly related to *G. spinifera* densities (Fig. 4d). The toxin concentration and causative microalgae density showed similar seasonal variation. Similar to *G. spinifera*, the concentrations of *D. acuminata* also showed a seasonal trend, which was highest in summer. Kim et al. (2010) reported that PTX concentrations in phytoplankton closely corresponded with the density of the causative microalgae. However, in the current study, PTX concentrations in phytoplankton showed no significant relationship with *D. acuminata* densities (Fig. 4d, $p > 0.05$). Thus, other causative microalgae of PTXs might exist on the southern coast of South Korea. *Dinophysis acuminata* could have been misidentified, because it is morphologically very similar to *D. sacculus* and *D. ovum*, which belong to the *D. acuminata* complex (Raho et al., 2008; Zingone et al., 1998). Thus, the causative microalgae of PTXs need to be investigated in detail in the future. Although no significant relationship was found between the density of causative microalgae and LMT concentrations of mussels in this study, a significant relationship was observed between LMT concentrations in phytoplankton and mussels. The concentration of YTX-producing microalgae is 0–200 pg $cell^{-1}$ (Howard et al., 2008), with mussels having filtration rates of 0.26–2.3 L h^{-1} (Denis et al., 1999). Thus, more YTX could be accumulated in mussels, even at low densities (i.e., <5 cells mL^{-1}). Overall, microalgae that produce LMTs were recorded on the southern coast of Korea during summer; consequently, LMTs accumulated in bivalves, raising concerns about the safety of aquatic products in this region.

Among the four target LMTs, homo-YTX was only detected in commercial shellfish samples. Homo-YTX was detected in seven samples (only for two species, red scallops and comb pen shells) out of a total of 121 samples (total 12 shellfish species) (Table 1). Concentrations of homo-YTX in red scallops and comb pen shells were <LOD–73 ng g^{-1} ww and <LOD–124 ng g^{-1} ww, respectively. Both red scallops and comb pen shells, in which homo-YTX were detected, were cultured in Yeosu and Tongyeong, which are located on the southern coast of South Korea. Previous studies reported that scallops accumulate relatively large amounts of biotoxins over relatively long time periods (Lee et al., 2012; Liu et al., 2019). This phenomenon might be attributed to scallops being larger than other shellfish, and due to higher feeding rates on phytoplankton (Li et al., 2015). In this study, the commercial shellfish samples in which LMTs were detected showed a temporal distribution (LMT concentrations were higher during summer), similar to those recorded in mussels collected from the southern coast. This similarity might be because shellfish are cultured in the South Sea, where samples were collected. In shellfish samples, LMTs (such as homo-YTX) were only detected in samples collected in September and October, and were not detected in any samples after October.

The maximum concentrations of YTXs were 73 ng YTX EQ g^{-1} ww and 124 ng YTX EQ g^{-1} ww in red scallops and comb pen shells, respectively. The concentrations of YTXs detected in seafood were lower than the 3.75 mg YTX EQ kg^{-1} ww suggested by EFSA (2008). To date, there has been no report of YTXs in domestic seafood, and regulation of YTXs has not been established in Korea. The exposure of YTXs to humans was calculated to evaluate the potential risks posed by the consumption of red scallops and comb pen shells. The mean and high consumption values of two contaminated bivalves by YTX and homo-YTX in the Korean database are shown in Table S10. The 95th and 97.5th percentile consumption rates of red scallops and comb pen shells were not available; instead, 2.5 and 3.0 times the mean of all participants were used to assess scenarios 3 and 4, respectively, following WHO guidance for dietary exposure assessment of chemical risk factors in food (WHO, 1985, 2020). Results indicated that no potential risk to human health was identified in the dietary exposure assessment of the two contaminated bivalve species (red scallops and comb pen shells) that had the highest homo-YTX concentrations (Table 2).

Comparison of the HQ% among scenarios revealed that food consumption is an important factor in estimating exposure levels. Even if the highest concentrations of homo-YTX in the comb pen shell are higher compared to red scallop, the consumption level of red scallop is around 8-fold higher compared to comb pen shell in South Korea. The range of dietary assessment on human consumption of these two contaminated

Table 2
Exposure to YTXs associated with the consumption of shellfish for the four tested scenarios in the human population of South Korea.

Species	Scenario	Dietary exposure (μg d^{-1})	HQ (%)	HI (%)[a]
Red scallop	S1	0.017	0.0012	0.0014
	S2	1.7	0.11	0.17
	S3	0.044	0.0029	0.0035
	S4	0.061	0.0041	0.005
Comb pen shell	S1	0.0037	0.0002	0.0014
	S2	0.86	0.058	0.17
	S3	0.0093	0.0006	0.0035
	S4	0.013	0.0009	0.005

[a] HI (%): sum of HQ for the two shellfish species in each scenario.

Table 1
Concentrations of LMTs in domestic shellfish collected from seafood markets. Out of 121 samples of 12 shellfish species, only those in which LMTs were detected were included in this table. A list of all tested samples is provided in Table S1 of the Supplementary Material.

Month	Seafood market	Origin	Species	YTX (ng g^{-1} ww)	Homo-YTX (ng g^{-1} ww)	PTX-2 (ng g^{-1} ww)	PTX-11 (ng g^{-1} ww)
September	Seoul	Tongyoung	Red scallop	<LOD[a]	73	<LOD	<LOD
	Daejeon	Yeosu	Comb pen shell	<LOD	121	<LOD	<LOD
	Busan	Tongyoung	Red scallop	<LOD	37	<LOD	<LOD
October	Seoul	Yeosu	Red scallop	<LOD	65	<LOD	<LOD
		Tongyoung	Red scallop	<LOD	63	<LOD	<LOD
		Yeosu	Comb pen shell	<LOD	124	<LOD	<LOD
	Busan	Tongyoung	Red scallop	<LOD	57	<LOD	<LOD

[a] <LOD: below limit of detection.

bivalve species was 0.037–1.7 μg d^{-1}, and an HQ% of over 100% was not observed in any scenario. Thus, the potential risk of consuming bivalves contaminated with YTXs is low in South Korea. In addition, because the HI% was below 1, exposure to toxic levels that could affect the health of consumers was low (Evans et al., 2015). Because there is a risk of chronic exposure to marine biotoxins, continuous monitoring for these toxins is required. Of importance, unmanaged marine biotoxins were detected in both coastal organisms on the southern coast and commercial shellfish in seafood markets.

In this study, YTXs and PTXs-producing phytoplanktons were observed at noticeably high densities along the southern coast of Korea during summer. YTXs and PTXs were detected in both phytoplankton and mussels, and concentrations were also greater during summer. In addition, homo-YTX was detected in domestic seafood, but not at a level considered to cause risk to human health. To date, there are no safety guidelines for LMTs, such as YTXs and PTXs, in seafood in Korea. Since LMT-producing microalgae frequently appear along the southern coast of Korea in summer, shellfish contamination by LMTs and chronic human exposure is possible. Therefore, continuous monitoring of LMTs is required, and preemptive management of these toxins.

CRediT authorship contribution statement

Mungi Kim: Conceptualization, Investigation, Formal analysis, Data curation, Visualization, Writing – original draft. **Seongjin Hong:** Conceptualization, Methodology, Writing – original draft, Writing – review & editing, Project administration, Funding acquisition, Supervision. **Young Kyun Lim:** Investigation, Formal analysis, Data curation. **Jihyun Cha:** Investigation, Formal analysis, Data curation. **Jiyun Gwak:** Investigation, Formal analysis, Data curation. **Youngnam Kim:** Investigation, Formal analysis, Data curation. **Seong-Ah An:** Investigation, Data curation. **Hee-seok Lee:** Investigation, Data curation, Writing – review & editing. **Seung Ho Baek:** Conceptualization, Investigation, Formal analysis, Data curation, Writing – review & editing.

Declaration of competing interest

The authors declare that they have no known competing financial interests or personal relationships that could have appeared to influence the work reported in this paper.

Acknowledgments

This research was supported by grant (20163MFDS641) from the Ministry of Food and Drug Safety, Korea. This research was also funded by the Ministry of Oceans and Fisheries, Korea (2014-0342).

Appendix A. Supplementary data

Supplementary data to this article can be found online at https://doi.org/10.1016/j.marpolbul.2022.113776.

References

Aasen, J., Samdal, I.A., Miles, C.O., Dahl, E., Briggs, L.R., Aune, T., 2005. Yessotoxins in norwegian blue mussels (Mytilus edulis): uptake from Protoceratium reticulatum, metabolism and depuration. Toxicon 45, 265–272.

Baek, S.H., Kim, D., Kim, Y.O., Son, M., Kim, Y.-J., Lee, M., Park, B.S., 2019. Seasonal changes in abiotic environmental conditions in the Busan coastal region (South Korea) due to the Nakdong River in 2013 and effect of these changes on phytoplankton communities. Cont. Shelf Res. 175, 116–126.

Baek, S.H., Kim, D., Son, M., Yun, S.M., Kim, Y.O., 2015. Seasonal distribution of phytoplankton assemblages and nutrient-enriched bioassays as indicators of nutrient limitation of phytoplankton growth in Gwangyang Bay, Korea. Estuar. Coast. Mar. Sci. 163, 265–278.

Baek, S.H., Lee, M., Park, B.S., Lim, Y.K., 2020. Variation in phytoplankton community due to an autumn typhoon and winter water turbulence in southern korean coastal waters. Sustainability 12, 2781.

Chang, P.-H., 2003. A numerical study on the changjiang diluted water in the yellow and East China seas. J. Geophys. Res. 108, 3299.

Chen, J., Li, X., Wang, S., Chen, F., Cao, W., Sun, C., Zheng, L., Wang, X., 2017. Screening of lipophilic marine toxins in marine aquaculture environment using liquid chromatography-mass spectrometry. Chemosphere 168, 32–40.

Denis, L., Alliot, E., Grzebyk, D., 1999. Clearance rate responses of Mediterranean mussels, Mytilus galloprovincialis, to variations in the flow, water temperature, food quality and quantity. Aquat. Living Rseour. 12, 279–288.

Draisci, R., Ferretti, E., Palleschi, L., Marchiafava, C., Poletti, R., Milandri, A., Ceredi, A., Pompei, M., 1999. High levels of yessotoxin in mussels and presence of yessotoxin and homoyessotoxin in dinoflagellates of the Adriatic Sea. Toxicon 37, 1187–1193.

Efsa, 2008. Scientific opinion of the panel on contaminants in the food chain on a request from the European Commission on marine biotoxins in shellfish–Yessotoxin group. EFSA J. 907, 1–62.

Efsa, 2009. Scientific opinion of the panel on contaminants in the food chain on a request from the European Commission on marine biotoxins in shellfish–Pectenotoxin group. EFSA J. 1109, 1–47.

Evans, R.M., Scholze, M., Kortenkamp, A., 2015. Examining the feasibility of mixture risk assessment: a case study using a tiered approach with data of 67 pesticides from the joint FAO/WHO meeting on pesticide residues (JMPR). Food Chem. Toxicol. 84, 260–269.

FAO/WHO, 2011. FAO/WHO guide for application of risk analysis principles and procedures during food safety emergencis. Rome. https://agris.fao.org/agris-search/search.do?recordID=XF2016018197.

Ferreiro, S.F., Vilarino, N., Carrera, C., Louzao, M.C., Cantalapiedra, A.G., Santamarina, G., Cifuentes, J.M., Vieira, A.C., Botana, L.M., 2016. Subacute cardiotoxicity of yessotoxin. In vitro and in vivo studies. Chem. Res. Toxicol. 29, 981–990.

Gerssen, A., Mulder, P.P., de Boer, J., 2011. Screening of lipophilic marine toxins in shellfish and algae: development of a library using liquid chromatography coupled to orbitrap mass spectrometry. Anal. Chim. Acta 685, 176–185.

Gobler, C.J., Doherty, O.M., Hattenrath-Lehmann, T.K., Griffith, A.W., Kang, Y., Litaker, R.W., 2017. Ocean warming since 1982 has expanded the niche of toxic algal blooms in the North Atlantic and North Pacific oceans. Proc. Natl. Acad. Sci. U. S. A. 114, 4975–4980.

Hallegraeff, G.M., Anderson, D.M., Belin, C., Bottein, M.-Y.D., Bresnan, E., Chinain, M., Enevoldsen, H., Iwataki, M., Karlson, B., McKenzie, C.H., Sunesen, I., Pitcher, G.C., Provoost, P., Richardson, A., Schweibold, L., Tester, P.A., Trainer, V.L., Yñiguez, A. T., Zingone, A., 2021. Perceived global increase in algal blooms is attributable to intensified monitoring and emerging bloom impacts. Commun. Earth Environ. 2, 117.

Howard, M.D.A., Silver, M., Kudela, R.M., 2008. Yessotoxin detected in mussel (Mytilus californicus) and phytoplankton samples from the U.S. West coast. Harmful Algae 7, 646–652.

Isobe, A., 1999. On the origin of the Tsushima warm current and its seasonality. Cont. Shelf Res. 19, 117–133.

Juan-Borrás, M., Domenech, E., Escriche, I., 2016. Mixture-risk-assessment of pesticide residues in retail polyfloral honey. Food Control 67, 127–134.

Kim, J.H., Lee, K.J., Suzuki, T., Kang, Y.S., Ho Kim, P., Song, K.C., Lee, T.S., 2010. Seasonal variability of lipophilic shellfish toxins in bivalves and waters, and abundance of Dinophysis spp. in Jinhae Bay, Korea. J. Shellfish Res. 29, 1061–1067.

Kim, J.H., Lee, M., Lim, Y.K., Kim, Y.J., Baek, S.H., 2019. Occurrence characteristics of harmful and non-harmful algal species related to coastal environments in the southern sea of Korea. Mar. Freshw. Res. 70, 794–806.

Korean Disease Control and Prevention Agency (KCDA), 2020. Available online at. https://www.kdca.go.kr/.

Lee, D.-H., Moon, S.-J., Kang, J.-H., 2019. A study on the evaluation and research status analysis of shellfish farming in southern coast of Korea. J. Fish. Bus. Adm. 50, 57–74.

Lee, K.J., Mok, J.S., Song, K.C., Yu, H., Lee, D.S., Jung, J.H., Kim, J.H., 2012. First detection and seasonal variation of lipophilic toxins okadaic acid, dinophysistoxin-1, and yessotoxin in korean gastropods. J. Food Prot. 75, 2000–2006.

Lee, M., Park, B.S., Baek, S.H., 2018. Tidal influences on biotic and abiotic factors in the Seomjin River Estuary and Gwangyang Bay, Korea. Estuar. Coast. 41, 1977–1993.

Li, A., Sun, G., Qiu, J., Fan, L., 2015. Lipophilic shellfish toxins in Dinophysis caudata picked cells and in shellfish from the East China Sea. Environ. Sci. Pollut. Res. 22, 3116–3126.

Li, M., Sun, G., Qiu, J., Li, A., 2017. Occurrence and variation of lipophilic shellfish toxins in phytoplankton, shellfish and seawater samples from the aquaculture zone in the Yellow Sea, China. Toxicon 127, 1–10.

Lim, Y.K., Baek, S.H., Lee, M., Kim, Y.O., Choi, K.-H., Kim, J.H., 2019. Phytoplankton composition associated with physical and chemical variables during summer in the southern sea of Korea: implication of the succession of the two toxic dinoflagellates cochlodinium (A.K.A. Margalefidinium) polykrikoides and Alexandrium affine. J. Exp. Mar. Biol. Ecol. 516, 51–66.

Lim, Y.K., Lee, G., Park, B.S., Cho, H.-Y., Choi, J.-Y., Baek, S.H., 2021. Differential responses of the dinoflagellate Cochlodinium polykrikoides bloom to episodic typhoon events. J. Appl. Phycol. 33, 2299–2311.

Liu, C., Ji, Y., Zhang, L., Qiu, J., Wang, Z., Liu, L., Zhuang, Y., Chen, T., Li, Y., Niu, B., Li, A., 2021. Spatial distribution and source of biotoxins in phytoplankton from the South China Sea, China. J. Hazard. Mater. 418, 126285.

Liu, Y., Yu, R.C., Kong, F.Z., Li, C., Dai, L., Chen, Z.F., Geng, H.X., Zhou, M.J., 2019. Contamination status of lipophilic marine toxins in shellfish samples from the Bohai Sea, China. Environ. Pollut. 249, 171–180.

Liu, Y., Yu, R.-C., Kong, F.-Z., Li, C., Dai, L., Chen, Z.-F., Zhou, M.-J., 2017. Lipophilic marine toxins discovered in the Bohai Sea using high performance liquid

chromatography coupled with tandem mass spectrometry. Chemosphere 183, 380–388.
MacKenzie, L., Holland, P., McNabb, P., Beuzenberg, V., Selwood, A., Suzuki, T., 2002. Complex toxin profiles in phytoplankton and greenshell mussels (Perna canaliculus), revealed by LC–MS/MS analysis. Toxicon 40, 1321–1330.
Ministry of Food and Drug Safety (MFDS), 2009. Regulatory limit for DSP in shellfish flesh. In: Notification Number 2009-24 of the Ministry of Food and Drug Safety. May 7.
Nielsen, L.T., Hansen, P.J., Krock, B., Vismann, B., 2016. Accumulation, transformation and breakdown of DSP toxins from the toxic dinoflagellate Dinophysis acuta in blue mussels, Mytilus edulis. Toxicon 117, 84–93.
Orellana, G., Vanden Bussche, J., Van Meulebroek, L., Vandegehuchte, M., Janssen, C., Vanhaecke, L., 2014. Validation of a confirmatory method for lipophilic marine toxins in shellfish using UHPLC-HR-orbitrap MS. Anal. Bioanal. Chem. 406, 5303–5312.
Paz, B., Daranas, A.H., Norte, M., Riobo, P., Franco, J.M., Fernandez, J.J., 2008. Yessotoxins, a group of marine polyether toxins: an overview. Mar. Drugs 6, 73–102.
Paz, B., Riobo, P., Ramilo, I., Franco, J.M., 2007. Yessotoxins profile in strains of Protoceratium reticulatum from Spain and USA. Toxicon 50, 1–17.
Pizarro, G., Escalera, L., González-Gil, S., Franco, J.M., Reguera, B., 2008. Growth, behaviour and cell toxin quota of Dinophysis acuta during a daily cycle. Mar. Ecol. Prog. Ser. 353, 89–105.
Raho, N., Pizarro, G., Escalera, L., Reguera, B., Marín, I., 2008. Morphology, toxin composition and molecular analysis of Dinophysis ovum Schütt, a dinoflagellate of the "Dinophysis acuminata complex". Harmful Algae 7, 839–848.
Ramstad, H., Larsen, S., Aune, T., 2001. Repeatability and validity of a fluorimetric HPLC method in the quantification of yessotoxin in blue mussels (Mytilus edulis) related to the mouse bioassay. Toxicon 39, 1393–1397.
Reguera, B., Riobo, P., Rodriguez, F., Diaz, P.A., Pizarro, G., Paz, B., Franco, J.M., Blanco, J., 2014. Dinophysis toxins: causative organisms, distribution and fate in shellfish. Mar. Drugs 12, 394–461.
Reguera, B., Velo-Suárez, L., Raine, R., Park, M.G., 2012. Harmful dinophysis species: a review. Harmful Algae 14, 87–106.
Satake, M., Ichimura, T., Sekiguchi, K., Yoshimatsu, S., Oshima, Y., 1999. Confirmation of yessotoxin and 45, 46, 47-trinoryessotoxin production by Protoceratium reticulatum collected in Japan. Nat. Toxins 7, 147–150.
Suzuki, T., Horie, Y., Koike, K., Satake, M., Oshima, Y., Iwataki, M., Yoshimatsu, S., 2007. Yessotoxin analogues in several strains of Protoceratium reticulatum in Japan determined by liquid chromatography-hybrid triple quadrupole/linear ion trap mass spectrometry. J. Chromatogr. A 1142, 172–177.
Terao, K., Ito, E., Ohkusu, M., Yasumoto, T., 1993. A comparative study of the effects of DSP-toxins on mice and rats. In: Toxic Phytoplankton Blooms in the Sea, 3, pp. 581–586.
Wang, Y., Chen, J., Li, Z., Wang, S., Shi, Q., Cao, W., Zheng, X., Sun, C., Wang, X., Zheng, L., 2015. Determination of typical lipophilic marine toxins in marine sediments from three coastal bays of China using liquid chromatography-tandem mass spectrometry after accelerated solvent extraction. Mar. Pollut. Bull. 101, 954–960.
WHO, 1985. Guidelines for the study of dietary intakes of chemical contaminants. In: WHO Offset Publication No. 87. World Health Organization, Geneva, pp. 1–100.
WHO, 2020. In: Chapter 6. Dietary Exposure Assessment for Chemicals in Food. World Health Organization, Geneva, pp. 1–177.
Yasumoto, T., 2005. Chemistry, etiology, and food chain dynamics of marine toxins. Proc. Jpn. Acad. Ser. B 81, 43–51.
Yoon, Y.H., Park, B., 2017. Biological oceanographic characteristics by the dinoflagellate cyst assemblages on the surface sediments in the Korea Coastal Waters (KCW). J. Korean Soc. Mar. Environ. Energy 20, 180–191.
Zingone, A., Montresor, M., Marino, D., 1998. Morphological variability of the potentially toxic dinoflagellate Dinophysis sacculus (Dinophyceae) and its taxonomic relationships with D. pavillardii and D. acuminata. Eur. J. Phycol. 33, 259–273.

<Marine Pollution Bulletin>

Supplementary materials for

Spatiotemporal distribution characteristics of yessotoxins and pectenotoxins in phytoplankton and shellfish collected from the southern coast of South Korea

Mungi Kim, Seongjin Hong*, Young Kyun Lim, Jihyun Cha, Jiyun Gwak, Youngnam Kim, Seong-Ah An, Hee-seok Lee, Seung Ho Baek*

This file includes:

Number of pages: 27

Number of Supplementary Tables: 10, Tables S1 to S10

Number of Supplementary Figures: 3, Figs. S1 to S3

***Corresponding authors.**

E-mail addresses: hongseongjin@cnu.ac.kr (S. Hong); baeksh@kiost.ac.kr (S.H. Baek).

Supplementary Tables

Table S1. Information on the domestic shellfish samples collected from three seafood markets in South Korea from September to December, 2020.

Month	Market	Common name	Scientific name	Origin	Shell length (cm)	Shell breadth (cm)
September 2020	Seoul (1)	Ark shell	*Scapharca subcrenata*	Beolgyo	3.4–4.1	2.7–3.2
		Red Shell	*Scapharca broughtonii*	Yeosu	5.1–5.9	3.9–4.8
		Mussel	*Mytilus galloprovincialis*	Yeosu	6.5–7.4	2.9–3.4
		Corb shell	*Cyclina sinensis*	Buan	3.4–4.2	3.1–3.9
		Surf clam	*Mactra veneriformis*	Buan	3.6–4.1	2.9–3.4
		Hard clam	*Meretrix lusoria*	Buan	7.9–8.6	6.5–7.1
		Purplish clam	*Saxidomus purpurata*	Yeosu	9.8–10.8	7.4–8
		Marsh clam	*Corbicula fluminea*	Namhae	2.5–3	2.3–2.6
		Comb pen shell	*Atrina pectinata*	Yeosu	23.1–25	11.7–12.8
		Red scallop	*Argopecten irradians*	Namhae	5.2–6.1	5.1–5.8
		Manila clam	*Ruditapes philippinarum*	Beolgyo	4.8–5.9	2.8–3.6
	Seoul (2)	Ark shell	*Scapharca subcrenata*	Beolgyo	3.4–4.1	2.7–3.2
		Red Shell	*Scapharca broughtonii*	Yeosu	5.1–5.9	3.9–4.8
		Corb shell	*Cyclina sinensis*	Buan	3.4–4.2	3.1–3.9
		Hard clam	*Meretrix lusoria*	Buan	7.7–8.6	6.6–7.1
		Purplish clam	*Saxidomus purpurata*	Yeosu	9.5–10.6	7.4–8.1
		Comb pen shell	*Atrina pectinata*	Yeosu	22.1–24	11.2–13
		Red scallop	*Argopecten irradians*	Tongyoung	4.2–6.3	5.3–5.8
		Manila clam	*Ruditapes philippinarum*	Yeosu	4.8–5.9	2.8–3.6
	Busan	Red Shell	*Scapharca broughtonii*	Yeosu	4.1–4.9	3.3–4.3
		Mussel	*Mytilus galloprovincialis*	Tongyoung	5.5–6.4	3.1–3.5
		Corb shell	*Cyclina sinensis*	Myeongji	3.4–4.2	3.1–3.9
		Hard clam	*Meretrix lusoria*	Myeongji	6.4–7.6	5.8–6.5
		Comb pen shell	*Atrina pectinata*	Yeosu	23.1–25	12.7–14
		Red scallop	*Argopecten irradians*	Tongyoung	5.2–6.3	5.1–5.8
		Manila clam	*Ruditapes philippinarum*	Myeongji	4.8–6.3	2.3–3.6
	Daejeon	Ark shell	*Scapharca subcrenata*	Yeosu	3.4–4.2	2.6–3.2
		Mussel	*Mytilus galloprovincialis*	Yeosu	5.5–6.4	3.2–3.5

		Corb shell	*Cyclina sinensis*	Buan	3.4–4.2	3.5–3.9
		Surf clam	*Mactra veneriformis*	Buan	3.6–4.1	2.4–3.4
		Comb pen shell	*Atrina pectinata*	Yeosu	21.1–23	11–13.4
		Manila clam	*Ruditapes philippinarum*	Namhae	4.8–5.9	2.8–4.1
October 2020	Seoul (1)	Ark shell	*Scapharca subcrenata*	Beolgyo	3.4–4.1	2.7–4.2
		Red Shell	*Scapharca broughtonii*	Yeosu	4.1–4.9	3.2–5.3
		Mussel	*Mytilus galloprovincialis*	Yeosu	5.5–6.4	3.3–4.5
		Corb shell	*Cyclina sinensis*	Buan	3.1–4.5	3.5–4.9
		Surf clam	*Mactra veneriformis*	Buan	4.6–6.1	3.1–3.9
		Hard clam	*Meretrix lusoria*	Buan	7.9–8.6	6.5–7.1
		Purplish clam	*Saxidomus purpurata*	Yeosu	9.7–10.8	7.5–8.1
		Marsh clam	*Corbicula fluminea*	Namhae	4.1–5.9	2.5–3.6
		Comb pen shell	*Atrina pectinata*	Yeosu	22.1–24	12.4–14.3
		Red scallop	*Argopecten irradians*	Yeosu	5.3–6.1	5.3–5.8
		Manila clam	*Ruditapes philippinarum*	Namhae	4.5–5.9	2.2–3.6
		Oyster	*Crassostrea gigas*	Tongyoung	7.7–8.1	5.2–6.1
	Seoul (2)	Ark shell	*Scapharca subcrenata*	Beolgyo	3.4–4.3	2.2–3.5
		Red Shell	*Scapharca broughtonii*	Yeosu	3.3–4.9	3.5–4.3
		Mussel	*Mytilus galloprovincialis*	Yeosu	5.6–6.4	3.7–3.5
		Corb shell	*Cyclina sinensis*	Buan	3.6–4.2	3.2–3.9
		Hard clam	*Meretrix lusoria*	Buan	7.7–8.6	6.1–7.2
		Purplish clam	*Saxidomus purpurata*	Yeosu	9.1–11	7.4–8.1
		Comb pen shell	*Atrina pectinata*	Yeosu	23.1–25	11.7–13.6
		Red scallop	*Argopecten irradians*	Tongyoung	5.2–6.3	5.2–5.8
		Manila clam	*Ruditapes philippinarum*	Yeosu	4.8–6.1	2.8–3.6
	Busan	Red Shell	*Scapharca broughtonii*	Namhae	4.1–5.1	3.3–4.2
		Mussel	*Mytilus galloprovincialis*	Tongyoung	5.5–6.8	2.9–3.5
		Corb shell	*Cyclina sinensis*	Myeongji	3.4–4.4	3.4–3.9
		Purplish clam	*Saxidomus purpurata*	Myeongji	9.8–10.8	7.4–8.6
		Comb pen shell	*Atrina pectinata*	Yeosu	23.1–25	13.7–14.8
		Red scallop	*Argopecten irradians*	Tongyoung	5.5–6.1	5.6–6.4
		Manila clam	*Ruditapes philippinarum*	Myeongji	5.2–5.9	2.8–3.6
November	Seoul (1)	Ark shell	*Scapharca subcrenata*	Beolgyo	3.7–4.3	2.5–3.3

2020		Red Shell	*Scapharca broughtonii*	Yeosu	3.8–4.4	4.1–4.5
		Mussel	*Mytilus galloprovincialis*	Yeosu	5.5–6.4	3.1–3.4
		Corb shell	*Cyclina sinensis*	Buan	3.4–4.2	3.1–3.8
		Surf clam	*Mactra veneriformis*	Buan	3.6–4.1	2.9–3.3
		Hard clam	*Meretrix lusoria*	Buan	7.9–8.6	6.4–7.3
		Purplish clam	*Saxidomus purpurata*	Yeosu	9.8–10.8	7.4–8.4
		Marsh clam	*Corbicula fluminea*	Namhae	2.5–3	2.3–3.1
		Comb pen shell	*Atrina pectinata*	Yeosu	23.1–26	11.6–14.2
		Red scallop	*Argopecten irradians*	Yeosu	5.2–6.5	5.3–6.1
		Manila clam	*Ruditapes philippinarum*	Namhae	4.5–5.9	2.8–3.6
		Oyster	*Crassostrea gigas*	Tongyoung	7.6–8.1	5.5–6.4
	Seoul (2)	Ark shell	*Scapharca subcrenata*	Beolgyo	3.4–4.1	2.7–3.5
		Mussel	*Mytilus galloprovincialis*	Yeosu	5.5–6.5	3.1–3.8
		Corb shell	*Cyclina sinensis*	Buan	3.4–4.2	3.6–4.2
		Surf clam	*Mactra veneriformis*	Buan	3.6–4.1	2.9–4.1
		Hard clam	*Meretrix lusoria*	Buan	7.9–8.6	6.5–8.3
		Purplish clam	*Saxidomus purpurata*	Yeosu	9.8–10.8	7.4–8.1
		Comb pen shell	*Atrina pectinata*	Yeosu	23.1–25	12.2–13.4
		Red scallop	*Argopecten irradians*	Tongyoung	5.2–6.1	5.1–5.8
		Manila clam	*Ruditapes philippinarum*	Yeosu	4.8–5.9	2.8–3.6
		Oyster	*Crassostrea gigas*	Tongyoung	7.6–8.1	5.5–6.1
	Busan	Ark shell	*Scapharca subcrenata*	Namhae	3.4–4.1	2.7–3.2
		Red Shell	*Scapharca broughtonii*	Namhae	4.1–4.9	3.1–4.3
		Mussel	*Mytilus galloprovincialis*	Myeongji	5.5–6.4	3.1–3.7
		Corb shell	*Cyclina sinensis*	Myeongji	3.1–4.2	3.2–3.9
		Purplish clam	*Saxidomus purpurata*	Myeongji	8.8–10.8	7.4–8
		Comb pen shell	*Atrina pectinata*	Myeongji	22.7–25	11.7–14
		Red scallop	*Argopecten irradians*	Tongyoung	5.1–6.1	5.1–7
		Manila clam	*Ruditapes philippinarum*	Jinhae	4.8–5.9	2.8–4.6
		Oyster	*Crassostrea gigas*	Tongyoung	7.6–8.1	5.5–7.1
December 2020	Seoul (1)	Ark shell	*Scapharca subcrenata*	Beolgyo	3.2–4.1	2.7–4.2
		Red Shell	*Scapharca broughtonii*	Yeosu	4.2–5.1	3.3–4.3
		Mussel	*Mytilus galloprovincialis*	Yeosu	5.1–6.4	3.2–3.7

	Corb shell	*Cyclina sinensis*	Buan	3.4–4.5	2.7–3.9
	Surf clam	*Mactra veneriformis*	Buan	3.1–4.5	2.9–3.4
	Hard clam	*Meretrix lusoria*	Buan	7.9–8.6	6.1–7.2
	Purplish clam	*Saxidomus purpurata*	Yeosu	9.4–11	7.4–8.1
	Comb pen shell	*Atrina pectinata*	Namhae	22–24.7	11–12.1
	Red scallop	*Argopecten irradians*	Yeosu	5.2–6.1	5.1–5.8
	Manila clam	*Ruditapes philippinarum*	Yeosu	4.8–5.9	2.8–3.6
	Oyster	*Crassostrea gigas*	Namhae	7.6–8.1	5.5–6.1
Seoul (2)	Ark shell	*Scapharca subcrenata*	Beolgyo	3.4–4.1	2.7–3.2
	Mussel	*Mytilus galloprovincialis*	Yeosu	5.5–6.4	3.1–3.5
	Corb shell	*Cyclina sinensis*	Buan	3.4–4.2	3.1–3.9
	Surf clam	*Mactra veneriformis*	Buan	2.8–4.1	2.9–3.4
	Purplish clam	*Saxidomus purpurata*	Yeosu	9.8–10.8	7.4–8
	Comb pen shell	*Atrina pectinata*	Yeosu	24.8–26.1	12.3–14.2
	Red scallop	*Argopecten irradians*	Tongyoung	5.4–6.1	5.1–5.8
	Manila clam	*Ruditapes philippinarum*	Yeosu	4.4–5.9	2.8–3.6
	Oyster	*Crassostrea gigas*	Tongyoung	7.4–8.1	5.5–6.1
Busan	Ark shell	*Scapharca subcrenata*	Namhae	3.3–4.1	2.7–3.2
	Red Shell	*Scapharca broughtonii*	Namhae	4.2–4.9	3.3–4.2
	Mussel	*Mytilus galloprovincialis*	Myeongji	5.3–6.3	3.1–3.5
	Corb shell	*Cyclina sinensis*	Myeongji	3.4–4.3	3.1–3.9
	Hard clam	*Meretrix lusoria*	Myeongji	7.9–8.8	6.5–7.1
	Purplish clam	*Saxidomus purpurata*	Myeongji	9.8–10.8	7.4–8
	Comb pen shell	*Atrina pectinata*	Myeongji	23.8–25.7	11–13.6
	Red scallop	*Argopecten irradians*	Tongyoung	5.5–6.9	5.0–5.7
	Manila clam	*Ruditapes philippinarum*	Jinhae	4.8–5.9	2.8–3.6
	Oyster	*Crassostrea gigas*	Tongyoung	7.6–8.1	5.5–6.1

Table S2. Instrumental conditions for the analysis of lipophilic marine biotoxins in biological samples using HPLC-MS/MS.

Instrument	HPLC: Agilent Infinity 1290 II MS/MS: Agilent 6470 triple quadrupole mass spectrometer		
Column	Waters X-Bridge C18, 3.0 mm × 150 mm, 5.0 µm		
Column temperature	25 ℃		
Mobile phase	(A): 0.05% NH_4OH in water, (B): 0.05% NH_4OH in 90% ACN		
Mobile phase gradient	Time (min)	Mobile phase	
		A (%)	B (%)
	0.0	70	30
	0.5	70	30
	4.0	45	55
	5.0	0	100
	8.0	0	100
	8.8	70	30
	10.0	70	30
Injection volume	5 µL		
Flow rate	0.4 mL min^{-1}		
Ion source	ESI (electrospray ionization)		
Polarity	Positive and negative		
Ion spray voltage	4000 V (positive) and -4500 V (negative)		
Gas temperature	350 ℃		
Sheath gas temperature	350 ℃		
Nebulizer gas	N_2 (25 psi)		
Sheath Gas	N_2 (11 psi)		

Table S3. Optimization of compound-specific parameters in a tandem mass spectrometer for the analysis of lipophilic marine biotoxins.

Compounds	Abbreviation	Molecular weight	MRM transition (ESI) Parent ion → Daughter ion (m/z)	Fragmentor (volts)	CE (volts)
Yessotoxin	YTX	1143.3	570.3 → 467.1	165	35
			→ 501.4 (ESI-)		25
Homo-yessotoxin	H-YTX	1157.4	577.2 → 472.2	165	32
			→ 508.8 (ESI-)		24
Pectenotoxin-2	PTX-2	859.07	876.5 → 823.4	176	26
			→ 841.4 (ESI+)		22
Pectenotoxin-11	PTX-11	875.05	892.4 → 839.2	173	26
			→ 821.3 (ESI+)		26

Table S4. Linear range, coefficient of determination (R^2), limit of detection (LOD), limit of quantification (LOQ), and spike test recovery of target marine biotoxins analyzed using LC-MS/MS.

Compounds	Linear range (ng mL^{-1})	R^2	LOD (ng g^{-1} ww)	LOQ (ng g^{-1} ww)	Recovery of spike test (n=4, mean±SD)	Coefficient of variation (n=4)
YTX	0–50	0.999	1.6	5.1	91±6	5.6
Homo-YTX	0–50	0.996	2.7	8.5	92±8	9.2
PTX-2	0–50	0.999	3.3	10.5	98±3	11
PTX-11	0–50	0.999	2.3	7.4	98±3	7.7

Table S5. Water quality parameters measured in the South Sea from June to December 2020.

Month	Site	WT[a] (°C)	DO (mg L^{-1})	Salinity (psu)	pH	Chl.a (μg L^{-1})	NO_2^-+NO_3^- (μM)	NH_4^+ (μM)	PO_4^{3-} (μM)	SiO_2 (μM)
Jun.	S1	19	8.4	33	8.1	0.64	1.5	0.86	0.08	6.4
	S2	20	7.8	33	8.1	2.4	5.04	3.5	0.6	16
	S3	21	7.9	33	8.1	0.54	0.79	1.4	0.201	5.2
	S4	-[b]	-	-	-	-	-	-	-	-
	S5	20	8.3	33	8.2	0.32	1.03	0.58	0.15	7.9
	S6	23	5.5	32	7.9	1.9	3.3	3.2	0.51	44
	S7	21	8.3	33	8.2	0.29	3.9	3.4	0.31	12
	S8	22	7.1	33	8.03	1.5	1.1	0.87	0.36	39
	S9	20	7.8	33	8.06	0.77	7.9	2.6	0.401	16
	S10	19	6.4	33	8	0.49	41	15	1.2	75
	S11	21	8.6	33	8.2	0.81	1.7	1.4	0.22	8.5
	S12	19	8.9	33	8.2	0.82	0.69	0.89	0.202	9.6
	S13	20	8.4	33	8.1	0.51	1.4	1.9	0.61	9.1
Jul.	S1	23	8.8	32	8.2	1.8	19	4.5	0.39	39
	S2	22	8.2	31	8.2	2.7	76	17	2.2	39
	S3	22	10.7	31	8.6	5.9	2.3	1.8	0.29	29
	S4	22	8.2	32	8.3	3.3	3.7	4.5	0.39	29
	S5	22	8.7	31	8.3	0.97	3.1	3.9	0.28	16
	S6	23	5.9	30.2	7.9	3.2	75	13	0.75	79
	S7	22	8.7	31	8.3	0.48	11	4.01	0.27	22
	S8	23	7.5	32	8.2	1.9	14	3.7	0.43	38
	S9	23	8.2	31	8.2	0.99	16	6.4	0.83	36
	S10	22	6.8	31	8.1	1.09	43	11	0.98	74
	S11	22	8.9	31	8.3	2.7	25	4.3	0.91	44
	S12	23	9.3	32	8.3	0.37	24	2.7	0.58	49
	S13	23	8.8	32	8.2	3.7	12	1.3	0.088	22
Aug.	S1	25	11	21	9.2	13	15	6.8	0.17	39
	S2	27	7.4	19	9.1	5.3	33	9.5	0.49	36
	S3	26	11	22	9.2	6.6	7.7	1.9	0.047	21
	S4	24	9.3	25	9	9.6	2.2	0.79	0.057	21
	S5	24	6.7	27	8.7	7.3	1.3	0.49	0.038	4.7
	S6	27	7.4	15	8.7	8.2	39	1.9	0.14	95
	S7	23	3.6	29	8.3	5.5	8.2	22	0.43	33
	S8	28	8.8	27	8.8	2.8	2.1	1.4	0.049	22
	S9	24	10.2	28	8.8	6.5	9.1	4.9	0.37	21
	S10	24	7.3	19	8.6	6.5	48	3.5	0.31	66
	S11	26	13	19	9.1	8.3	36	5.5	0.31	50
	S12	25	10.1	30	8.9	2.6	4.3	5.7	0.19	25
	S13	24	11	28	8.9	6.5	1.5	1.4	0.12	5.6
Sep.	S1	26	7.2	30	8.3	4.8	8.1	2.3	0.35	16
	S2	27	7.4	30	8.3	3.6	6.6	7.6	0.84	11
	S3	25	6.8	30	8.2	0.87	5.8	5.4	0.65	17
	S4	26	6.4	28	8.3	2.2	13	4.4	0.45	20.1
	S5	27	7.9	30.4	8.3	2.03	3.6	2.8	0.27	6.3
	S6	-	-	-	-	-	-	-	-	-
	S7	28	7.1	30	8.3	1.9	2.3	0.89	0.058	11
	S8	26	7.03	30	8.2	5.6	9.9	0.37	0.22	23

Table S5. Continued.

Month	Site	WT[a] (°C)	DO (mg L^{-1})	Salinity (psu)	pH	Chl.a (μg L^{-1})	NO_2^-+NO_3^- (μM)	NH_4^+ (μM)	PO_4^{3-} (μM)	SiO_2 (μM)
Sep.	S9	26	6.4	32	8.1	4.6	8.5	8.4	0.72	26
	S10	23	4.3	31	7.9	3.5	8.8	7.2	0.74	37
	S11	25	6.3	31	8.1	3.3	8.9	7.4	0.58	22
	S12	26	7.03	32	8.3	1.8	4.2	3.4	0.27	21
	S13	26	11	31	8.4	7.1	1.7	0.69	0.055	11
Oct.	S1	22	6.5	32	8.3	1.3	6.1	5.1	0.65	13
	S2	22	6.9	31	8.4	3.5	3.3	5.9	0.58	5.4
	S3	22	6.7	31	8.2	5.5	1.9	0.72	0.61	5.5
	S4	21	6.1	32	8.2	0.43	8.02	8.7	0.89	18
	S5	22	6.02	31	8.2	6.6	1.5	0.46	0.29	3.6
	S6	22	4.3	30	7.9	1.6	7.2	11	1.4	52
	S7	22	7.3	31	8.2	5.5	1.1	0.037	0.22	1.5
	S8	23	6.7	32	8.3	2.8	1.3	0.39	0.64	15
	S9	23	5.8	32	8.3	0.64	5.8	4.5	0.96	17
	S10	23	6.5	31	8.4	1.3	3.8	7.4	0.71	8.5
	S11	22	6.5	32	8.4	0.89	3.9	9.9	0.9	16
	S12	23	6.7	32	8.5	1.3	4.2	3.3	0.54	16
	S13	23	7.1	32	8.4	5.5	3.9	2.5	0.54	12
Nov.	S1	18	7.4	34	8.2	2.4	4.2	2.2	0.42	5.5
	S2	18	7.3	33	8.1	2.3	7.5	5.2	0.78	12
	S3	18	7.03	33	8.2	1.5	2.6	5.5	0.92	9.6
	S4	18	8.0	33	8.2	0.96	4.8	6.8	0.65	6.2
	S5	18	7.4	32	8.1	0.0602	2.3	2.2	0.66	4.2
	S6	18	6.9	32	8.03	0.67	5.2	4.7	0.89	28
	S7	18	7.9	32	8.1	2.5	0.65	0.0072	0.28	1.9
	S8	18	7.8	33	8.2	3.1	0.68	0.21	0.29	5.7
	S9	19	6.5	33	8.1	0.602	7.01	4.05	0.84	21
	S10	19	6.4	33	8.1	2.4	7.6	9.6	0.89	20
	S11	19	6.9	33	8.2	2.2	12	4.3	0.86	18
	S12	19	6.8	34	8.2	1.2	3.8	2.2	0.35	11
	S13	19	6.6	33	8.2	5.2	17	7.8	1.2	27
Dec.	S1	13	7.7	35	8.1	0.56	10.4	2.9	0.73	18
	S2	11	8.3	34	8.2	0.38	11	5.9	0.73	18
	S3	12	8.3	34	8.2	0.39	6.4	2.9	0.82	21
	S4	12	8.3	34	8.2	0.19	10.03	4.4	0.93	19
	S5	13	7.5	34	8.2	0.31	8.7	5.01	0.87	22
	S6	10.3	7.8	33	8.04	0.66	11	3.7	0.95	39
	S7	13	8.3	34	8.1	0.39	2.9	3.5	0.59	12
	S8	9.9	9.4	34	8.1	0.67	1.4	1.5	0.45	23
	S9	13	8.2	34	8.2	0.26	8.9	4.7	0.89	21
	S10	13	7.7	34	8.2	0.19	12	10.6	1.2	29
	S11	13	7.9	35	8.2	0.26	12	3.5	0.81	20
	S12	14	7.6	35	8.2	0.39	10.2	1.1	0.67	18
	S13	13	7.9	34	8.2	0.47	6.2	3.3	0.64	17

[a]WT: Water temperature.
[b]-: Not measured.

Table S6. Density of phytoplankton identified in the South Sea (S1–S13) from June to December 2020.

Month	Site	Bacillariophyceae (cells mL^{-1})	Dinophyceae (cells mL^{-1})	Cryptophyceae (cells mL^{-1})	Dictyochophyceae (cells mL^{-1})	Raphidophyceae (cells mL^{-1})	Others (cells mL^{-1})	Total (cells mL^{-1})
Jun.	S1	106	36	51	0	0	0	193
	S2	415	76	113	1.6	0	0	606
	S3	119	7.5	20	0	0	0	146
	S4	-[a]	-	-	-	-	-	-
	S5	89	13	12	0	0	0	114
	S6	24	11	80	0	0	0	115
	S7	45	11	345	0	0	0	401
	S8	342	17	190	0	0	0	550
	S9	199	41	290	0	0	0	530
	S10	102	15	17	0	0	0	134
	S11	143	26	45	0	0	0	214
	S12	39	66	30.1	0	0	0	135
	S13	304	16	29	0	0	0	350
Jul.	S1	0	97	65	3.2	0	0	166
	S2	1539	65	16	0.92	0	0	1622
	S3	137	200	64	0.94	0	0	402
	S4	3.9	13	13	0	0	0	30
	S5	9.01	3.6	14	0	0	0	26
	S6	0.87	0.87	29	0	0	0	30.3
	S7	12	8.3	7.4	0	0	0	27
	S8	1752	8.3	67	0	0	0	1827
	S9	32	3.7	57	0	0	0	92
	S10	47	8.4	30	0.93	0	0	86
	S11	118	13	18	0	0	0	148
	S12	4.8	8.7	19	0	0	0	33
	S13	1211	21	147	0	0	0	1379
Aug.	S1	5004	15	17	0.91	0	0	5037
	S2	2730	12	17	0	0	0	2759
	S3	2723	12	178	0	0	0	2913

[a]-: Sample was not collected.

Table S6. Continued.

Month	Site	Bacillariophyceae (cell mL^{-1})	Dinophyceae (cell mL^{-1})	Cryptophyceae (cell mL^{-1})	Dictyochophyceae (cell mL^{-1})	Raphidophyceae (cell mL^{-1})	Others (cell mL^{-1})	Total (cell mL^{-1})
Aug.	S4	5191	0	40	0	0	0	5230
	S5	3013	0.94	79	0	0	0	3093
	S6	341	21	391	0	0	0	754
	S7	670	8.5	89	3.4	0	0	771
	S8	109	42	35	0	0	0	187
	S9	744	378	47	1.9	0	0	1172
	S10	2502	55	133	0	0	0	2670
	S11	1019	498	430	0.89	0	0	1948
	S12	6.1	41	13	7.9	0	0	69
	S13	333	123	25	6.5	0	0	489
Sep.	S1	96	37	49	0	3.9	0	185
	S2	107	102	0	0	0.84	0	210
	S3	6.3	6.3	1.8	0	1.8	0	16
	S4	45	5.04	1.7	0	1.7	0	54
	S5	353	2.8	0	0	0	0	356
	S6	-[a]	-	-	-	-	-	-
	S7	290	23	10.4	0	0.95	0	324
	S8	2344	40.3	0	0	0	0	2385
	S9	41	44	0	0.89	30.3	0	116
	S10	491	6.2	0	1.8	0	0	499
	S11	318	11	0	0	0	0	329
	S12	18	42	0	0	0.91	0	61
	S13	3733	25	1.6	0	0	0	3760
Oct.	S1	134	7.5	2.5	0	0	0	144
	S2	234	1.8	1.8	0	0	0	237
	S3	809	2.6	0	0	0	0	811
	S4	28	2.6	10.2	0	0	0	41
	S5	623	14	1.9	0	0	0	638
	S6	64	7.8	31	0	0	0	103

[a]-: Sample was not collected.

Table S6. Continued.

Month	Site	Bacillariophyceae (cell mL^{-1})	Dinophyceae (cell mL^{-1})	Cryptophyceae (cell mL^{-1})	Dictyochophyceae (cell mL^{-1})	Raphidophyceae (cell mL^{-1})	Others (cell mL^{-1})	Total (cell mL^{-1})
Oct.	S7	1281	1.6	0	0	0	0	1282
	S8	284	1.7	13	0	0	0	299
	S9	102	7.7	25	0	0	0	135
	S10	44	7.5	34	0	0	0	86
	S11	9.6	34	4.8	0	0	0	48
	S12	5.7	22	52	0	0	0	80
	S13	103	154	7.05	0.88	0.88	0	266
Nov,	S1	204	5.05	13	0	0	0	222
	S2	163	2.6	19	0	0	0	184
	S3	104	3.9	1.6	0	0	0	109
	S4	58	3.7	0	0	0	0	62
	S5	129	2.8	2.8	0	0	0	135
	S6	22	0.80	10.4	1.6	0	0	35
	S7	226	0	27	0	0	0	253
	S8	582	4.3	10.2	0	0	0	597
	S9	2.8	0.92	4.6	0	0	0	8.3
	S10	42	4.7	19	0	0	0	65
	S11	4.6	22	257	0	0	0	284
	S12	4.5	4.5	13	0	0	0	22
	S13	7.1	108	858	0	0	0	973
Dec.	S1	38	9.05	511	1.8	0	0	559
	S2	20.2	3.5	29	0	0	0	53
	S3	25	2.7	117	0	0	0	145
	S4	18	5.4	59	0	0	0	82
	S5	33	0.93	29	0	0	0	62
	S6	3.6	0.90	711	0	0	0	715
	S7	44	4.1	346	0	0	0	394
	S8	263	5.5	154	0	0	0	422
	S9	3.8	7.6	55	0	0	0	67
	S10	4.3	4.3	59	0	0	0	68

Table S6. Continued.

Month	Site	Bacillariophyceae (cell mL^{-1})	Dinophyceae (cell mL^{-1})	Cryptophyceae (cell mL^{-1})	Dictyochophyceae (cell mL^{-1})	Raphidophyceae (cell mL^{-1})	Others (cell mL^{-1})	Total (cell mL^{-1})
Dec.	S11	7.8	12	205	0	0	0	225
	S12	13	14	100	0	0	0	128
	S13	125	1.9	22	0	0	0	149

Table S7. Abundance of causative microalgae of marine biotoxins collected from the South Sea from June to December 2020.

Month	Site	*Pseudo-nitzschia* spp. (cells L^{-1})	*Alexandrium* spp. (cells L^{-1})	*G. spinifera* (cells L^{-1})	*D. acuminata* (cells L^{-1})
Jun.	S1	60700	4200	1700	ND[a]
	S2	334000	1600	10500	810
	S3	22430	830	ND	ND
	S4	ND	ND	ND	ND
	S5	16800	930	1900	ND
	S6	9200	ND	ND	840
	S7	19200	ND	1600	ND
	S8	330000	890	4500	ND
	S9	181000	3200	800	ND
	S10	70940	690	2800	ND
	S11	12500	1800	5300	ND
	S12	13800	2600	1700	860
	S13	193000	260	ND	ND
Jul.	S1	ND	ND	3200	810
	S2	5500	ND	920	ND
	S3	17900	1900	1900	ND
	S4	790	ND	ND	ND
	S5	ND	ND	ND	ND
	S6	870	ND	870	ND
	S7	ND	ND	ND	ND
	S8	143400	ND	ND	1030
	S9	13700	ND	910	ND
	S10	2800	ND	930	ND
	S11	7500	ND	ND	ND
	S12	ND	ND	ND	ND
	S13	125000	1600	3200	ND
Aug.	S1	718000	ND	5500	ND
	S2	39100	ND	3300	810
	S3	850800	ND	ND	ND
	S4	569000	ND	ND	ND
	S5	1465000	ND	ND	ND
	S6	17000	ND	4300	ND
	S7	254000	170	ND	1700
	S8	49000	ND	940	ND
	S9	36500	1900	20000	ND
	S10	56600	ND	910	ND
	S11	5350	ND	5400	ND
	S12	880	ND	ND	ND
	S13	121000	ND	1900	930

[a]ND: Not detection.

Table S7. Continued.

Month	Site	*Pseudo-nitzschia* spp. (cells L^{-1})	*Alexandrium* spp. (cells L^{-1})	*G. spinifera* (cells L^{-1})	*D. acuminata* (cells L^{-1})
Sep.	S1	32000	800	800	ND[a]
	S2	ND	ND	ND	ND
	S3	4500	ND	ND	ND
	S4	42900	ND	ND	840
	S5	1800	ND	ND	ND
	S6	ND	ND	ND	ND
	S7	ND	950	950	ND
	S8	726000	11000	6300	ND
	S9	7100	8900	3600	ND
	S10	345800	ND	890	ND
	S11	128900	5600	ND	ND
	S12	11800	10000	ND	ND
	S13	2328000	2400	ND	ND
Oct.	S1	19000	ND	ND	ND
	S2	23000	ND	ND	ND
	S3	136000	ND	ND	ND
	S4	6800	ND	ND	ND
	S5	91000	930	928	ND
	S6	6040	ND	ND	1700
	S7	211000	ND	ND	ND
	S8	61300	ND	860	ND
	S9	3800	ND	ND	ND
	S10	5030	ND	ND	ND
	S11	ND	ND	ND	ND
	S12	950	ND	ND	ND
	S13	4400	15000	ND	ND
Nov.	S1	4200	ND	ND	ND
	S2	860	ND	ND	ND
	S3	5500	ND	800	ND
	S4	4600	ND	ND	ND
	S5	3800	ND	ND	ND
	S6	ND	ND	ND	ND
	S7	41500	ND	ND	ND
	S8	14500	1700	ND	ND
	S9	ND	ND	ND	ND
	S10	ND	ND	ND	ND
	S11	920	11000	920	ND
	S12	3600	910	ND	ND
	S13	4500	91500	4500	890

[a]ND: Not detection.

Table S7. Continued.

Month	Site	*Pseudo-nitzschia* spp. (cells L^{-1})	*Alexandrium* spp. (cells L^{-1})	*G. spinifera* (cells L^{-1})	*D. acuminata* (cells L^{-1})
Dec.	S1	3600	910	910	ND[a]
	S2	890	ND	ND	ND
	S3	900	ND	ND	ND
	S4	1800	ND	ND	ND
	S5	930	ND	ND	ND
	S6	1800	ND	ND	ND
	S7	5000	ND	ND	ND
	S8	185000	ND	ND	ND
	S9	ND	ND	ND	ND
	S10	ND	ND	ND	ND
	S11	3500	ND	ND	ND
	S12	ND	ND	ND	ND
	S13	2800	ND	ND	ND

[a]ND: Not detection.

Table S8. YTXs and PTXs concentrations in phytoplankton collected from the South Sea from June to December 2020.

Month	Site	YTX (ng g^{-1} ww)	Homo-YTX (ng g^{-1} ww)	PTX-2 (ng g^{-1} ww)	PTX-11 (ng g^{-1} ww)
Jun.	S1	<LOD[a]	111	<LOD	<LOD
	S2	<LOD	473	5.9	<LOD
	S3	<LOD	91	<LOD	<LOD
	S4	<LOD	<LOD	<LOD	<LOD
	S5	<LOD	91	<LOD	<LOD
	S6	<LOD	<LOD	29	<LOD
	S7	<LOD	<LOD	<LOD	<LOD
	S8	<LOD	<LOD	<LOD	<LOD
	S9	<LOD	65	<LOD	<LOD
	S10	<LOD	<LOD	<LOD	<LOD
	S11	<LOD	138	<LOD	<LOD
	S12	<LOD	5714	11	<LOD
	S13	<LOD	314	17	<LOD
Jul.	S1	<LOD	123	21	<LOD
	S2	<LOD	33	9.6	<LOD
	S3	<LOD	55	<LOD	<LOD
	S4	<LOD	267	44	<LOD
	S5	<LOD	232	17	<LOD
	S6	<LOD	<LOD	<LOD	<LOD
	S7	<LOD	<LOD	<LOD	<LOD
	S8	<LOD	<LOD	<LOD	<LOD
	S9	<LOD	903	58	<LOD
	S10	<LOD	<LOD	21	<LOD
	S11	<LOD	<LOD	<LOD	<LOD
	S12	<LOD	195	38	<LOD
	S13	<LOD	96	26	<LOD
Aug.	S1	<LOD	<LOD	105	78
	S2	<LOD	132	201	182
	S3	<LOD	62	96	19
	S4	<LOD	45	<LOD	<LOD
	S5	<LOD	24	9.6	<LOD
	S6	<LOD	<LOD	<LOD	3.5
	S7	<LOD	<LOD	61	14
	S8	<LOD	<LOD	<LOD	<LOD
	S9	<LOD	<LOD	12	<LOD
	S10	<LOD	<LOD	14	<LOD
	S11	<LOD	<LOD	11	<LOD
	S12	<LOD	239	27	<LOD
	S13	<LOD	<LOD	6.4	<LOD

[a]<LOD: Below limit of detection.

Table S8. Continued.

Month	Site	YTX (ng g^{-1} ww)	Homo-YTX (ng g^{-1} ww)	PTX-2 (ng g^{-1} ww)	PTX-11 (ng g^{-1} ww)
Sep.	S1	<LOD[a]	<LOD	18	<LOD
	S2	<LOD	<LOD	<LOD	<LOD
	S3	<LOD	<LOD	<LOD	<LOD
	S4	<LOD	<LOD	17	<LOD
	S5	<LOD	<LOD	<LOD	5.03
	S6	<LOD	<LOD	<LOD	<LOD
	S7	<LOD	<LOD	<LOD	<LOD
	S8	<LOD	303	<LOD	<LOD
	S9	<LOD	<LOD	26	<LOD
	S10	<LOD	<LOD	<LOD	<LOD
	S11	<LOD	<LOD	11.	<LOD
	S12	<LOD	<LOD	9.8	<LOD
	S13	<LOD	<LOD	13	<LOD
Oct.	S1	<LOD	<LOD	5.9	<LOD
	S2	<LOD	<LOD	<LOD	<LOD
	S3	<LOD	<LOD	23	<LOD
	S4	<LOD	<LOD	<LOD	<LOD
	S5	<LOD	<LOD	8.1	<LOD
	S6	<LOD	<LOD	426	21.8796
	S7	<LOD	<LOD	<LOD	<LOD
	S8	<LOD	<LOD	<LOD	<LOD
	S9	<LOD	<LOD	<LOD	<LOD
	S10	<LOD	<LOD	<LOD	<LOD
	S11	<LOD	<LOD	<LOD	<LOD
	S12	<LOD	<LOD	<LOD	<LOD
	S13	<LOD	<LOD	19	<LOD
Nov.	S1	<LOD	<LOD	1.3	<LOD
	S2	<LOD	<LOD	10.3	<LOD
	S3	<LOD	<LOD	32	1.5533
	S4	<LOD	<LOD	<LOD	<LOD
	S5	<LOD	<LOD	4.7	<LOD
	S6	<LOD	<LOD	<LOD	<LOD
	S7	<LOD	<LOD	<LOD	<LOD
	S8	<LOD	<LOD	<LOD	<LOD
	S9	<LOD	<LOD	<LOD	<LOD
	S10	<LOD	<LOD	2.6	<LOD
	S11	<LOD	<LOD	17	<LOD
	S12	<LOD	<LOD	15	<LOD
	S13	<LOD	<LOD	33	<LOD

[a]<LOD: Below limit of detection.

Table S8. Continued.

Month	Site	YTX (ng g^{-1} ww)	Homo-YTX (ng g^{-1} ww)	PTX-2 (ng g^{-1} ww)	PTX-11 (ng g^{-1} ww)
Dec.	S1	<LOD[a]	<LOD	16	<LOD
	S2	<LOD	<LOD	11	<LOD
	S3	<LOD	<LOD	3.6	<LOD
	S4	<LOD	<LOD	13	<LOD
	S5	<LOD	<LOD	2.6	<LOD
	S6	<LOD	<LOD	<LOD	<LOD
	S7	<LOD	<LOD	9.2	<LOD
	S8	<LOD	<LOD	<LOD	<LOD
	S9	<LOD	<LOD	6.5	<LOD
	S10	<LOD	<LOD	6.8	<LOD
	S11	<LOD	<LOD	18	<LOD
	S12	<LOD	<LOD	<LOD	<LOD
	S13	<LOD	<LOD	2.5	<LOD

[a]<LOD: Below limit of detection.

Table S9. YTXs and PTXs concentrations in mussels collected from the South Sea from June to December 2020.

Month	Site	YTX (ng g^{-1} ww)	Homo-YTX (ng g^{-1} ww)	PTX-2 (ng g^{-1} ww)	PTX-11 (ng g^{-1} ww)
Jun.	S1	<LOD[a]	<LOD	<LOD	<LOD
	S2	<LOD	153	<LOD	<LOD
	S3	<LOD	51	<LOD	<LOD
	S4	NS[b]	NS	NS	NS
	S5	30.2	54	<LOD	<LOD
	S6	<LOD	<LOD	<LOD	<LOD
	S7	41	50	<LOD	<LOD
	S8	<LOD	22	<LOD	<LOD
	S9	<LOD	239	<LOD	<LOD
	S10	83	54	<LOD	<LOD
	S11	<LOD	191	<LOD	<LOD
	S12	<LOD	859	<LOD	<LOD
	S13	<LOD	784	<LOD	<LOD
Jul.	S1	22	123	<LOD	<LOD
	S2	27	436	<LOD	<LOD
	S3	<LOD	248	<LOD	<LOD
	S4	15	770	<LOD	<LOD
	S5	21	636	<LOD	<LOD
	S6	<LOD	ND	<LOD	<LOD
	S7	26	77	<LOD	<LOD
	S8	<LOD	79	<LOD	<LOD
	S9	<LOD	696	<LOD	<LOD
	S10	39	502	<LOD	<LOD
	S11	<LOD	555	<LOD	<LOD
	S12	<LOD	1051	<LOD	<LOD
	S13	<LOD	412	<LOD	<LOD
Aug.	S1	23	152	<LOD	<LOD
	S2	21	93	<LOD	<LOD
	S3	<LOD	110	<LOD	<LOD
	S4	<LOD	92	<LOD	<LOD
	S5	<LOD	84	<LOD	<LOD
	S6	NS	NS	NS	NS
	S7	<LOD	<LOD	<LOD	<LOD
	S8	<LOD	91	<LOD	<LOD
	S9	<LOD	305	<LOD	<LOD
	S10	<LOD	60	<LOD	<LOD
	S11	<LOD	215	<LOD	<LOD
	S12	<LOD	414	<LOD	<LOD
	S13	<LOD	360	<LOD	<LOD

[a]<LOD: Below limit of detection.
[b]NS: Not sampled.

Table S9. Continued.

Month	Site	YTX (ng g^{-1} ww)	Homo-YTX (ng g^{-1} ww)	PTX-2 (ng g^{-1} ww)	PTX-11 (ng g^{-1} ww)
Sep.	S1	<LOD[a]	55	<LOD	<LOD
	S2	<LOD	58	<LOD	<LOD
	S3	NS[b]	NS	NS	NS
	S4	<LOD	130	<LOD	<LOD
	S5	<LOD	115	<LOD	<LOD
	S6	NS	NS	NS	NS
	S7	24	<LOD	<LOD	<LOD
	S8	<LOD	<LOD	<LOD	<LOD
	S9	<LOD	30.3	<LOD	<LOD
	S10	NS	NS	NS	NS
	S11	NS	NS	NS	NS
	S12	NS	NS	NS	NS
	S13	<LOD	97	<LOD	<LOD
Oct.	S1	<LOD	<LOD	<LOD	<LOD
	S2	<LOD	245.0	<LOD	<LOD
	S3	<LOD	114	<LOD	<LOD
	S4	<LOD	<LOD	<LOD	<LOD
	S5	NS	NS	NS	NS
	S6	NS	NS	NS	NS
	S7	14	54	<LOD	<LOD
	S8	<LOD	64	<LOD	<LOD
	S9	<LOD	74	<LOD	<LOD
	S10	<LOD	<LOD	<LOD	<LOD
	S11	NS	NS	NS	NS
	S12	<LOD	47	<LOD	<LOD
	S13	<LOD	184	<LOD	<LOD
Nov.	S1	20.4	37	<LOD	<LOD
	S2	20	59	<LOD	<LOD
	S3	20.2	139	<LOD	<LOD
	S4	NS	NS	NS	NS
	S5	20	29	<LOD	<LOD
	S6	NS	NS	NS	NS
	S7	20	57	<LOD	<LOD
	S8	18	55	<LOD	<LOD
	S9	19	52	<LOD	<LOD
	S10	NS	NS	NS	NS
	S11	NS	NS	NS	NS
	S12	20	45	<LOD	<LOD
	S13	20	226	<LOD	<LOD

[a]<LOD: Below limit of detection.
[b]NS: Not sampled.

Table S9. Continued.

Month	Site	YTX (ng g^{-1} ww)	Homo-YTX (ng g^{-1} ww)	PTX-2 (ng g^{-1} ww)	PTX-11 (ng g^{-1} ww)
Dec.	S1	21	29	<LOD[a]	<LOD
	S2	19	73	<LOD	<LOD
	S3	19	143	<LOD	<LOD
	S4	19	45	<LOD	<LOD
	S5	19	18	<LOD	<LOD
	S6	NS[b]	NS	NS	NS
	S7	20	21	<LOD	<LOD
	S8	19	51	<LOD	<LOD
	S9	18	29	<LOD	<LOD
	S10	NS	NS	NS	NS
	S11	20	34	<LOD	<LOD
	S12	18	117	<LOD	<LOD
	S13	19	48	<LOD	<LOD

[a]<LOD: Below limit of detection.
[b]NS: Not sampled.

Table S10. Consumption rates of two bivalve species (red scallop and comb pen shell) contaminated by YTX and homo-YTX in South Korea.

Species	Food consumption rates (g d^{-1}) in KNHANES (2016–2018)			
	All participants			Only consumers
	Mean	95th[a]	97.5th[b]	mean
Red scallop	0.24	-[c]	-	23.73
Comb pen shell	0.03	-	-	6.97

[a] If the 95th level was not available, 2.5 times the mean of all participants was used to assess scenario 3 by recommendation from WHO.

[b] If the 97.5th level was not available, 3.0 times the mean of all participants was used to assess scenario 4 by recommendation from WHO.

[c] not available.

Supplementary Figures

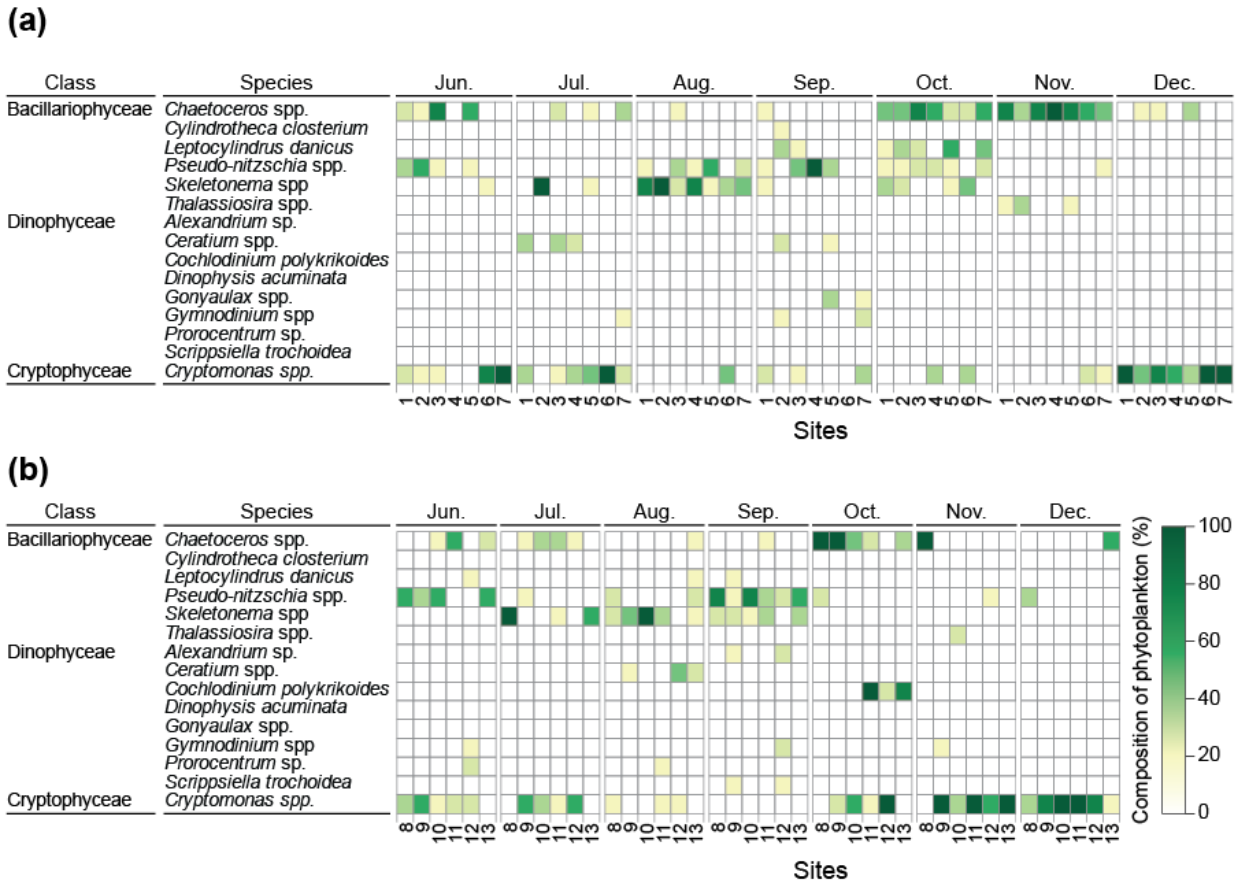

Fig. S1. Relative composition of the 15 most abundant phytoplankton species in **(a)** Group 1 and **(b)** Group 2 on the southern coast of South Korea.

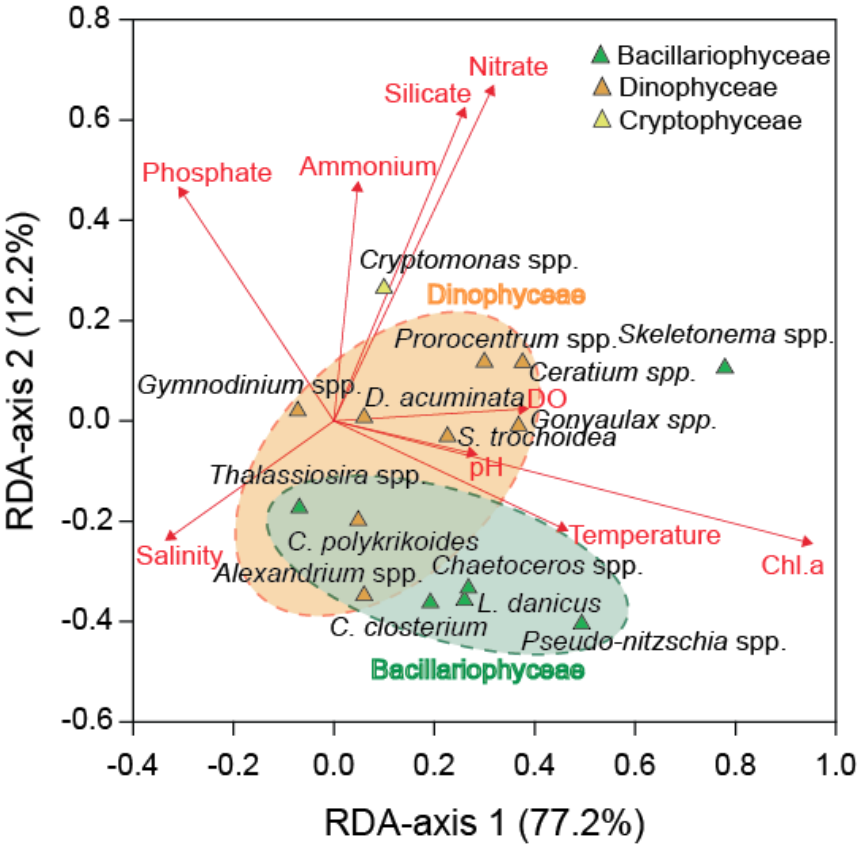

Fig. S2. Redundancy analysis (RDA) of the relationship between environmental parameters (red arrow) and population of phytoplankton (triangle) in treatment groups.

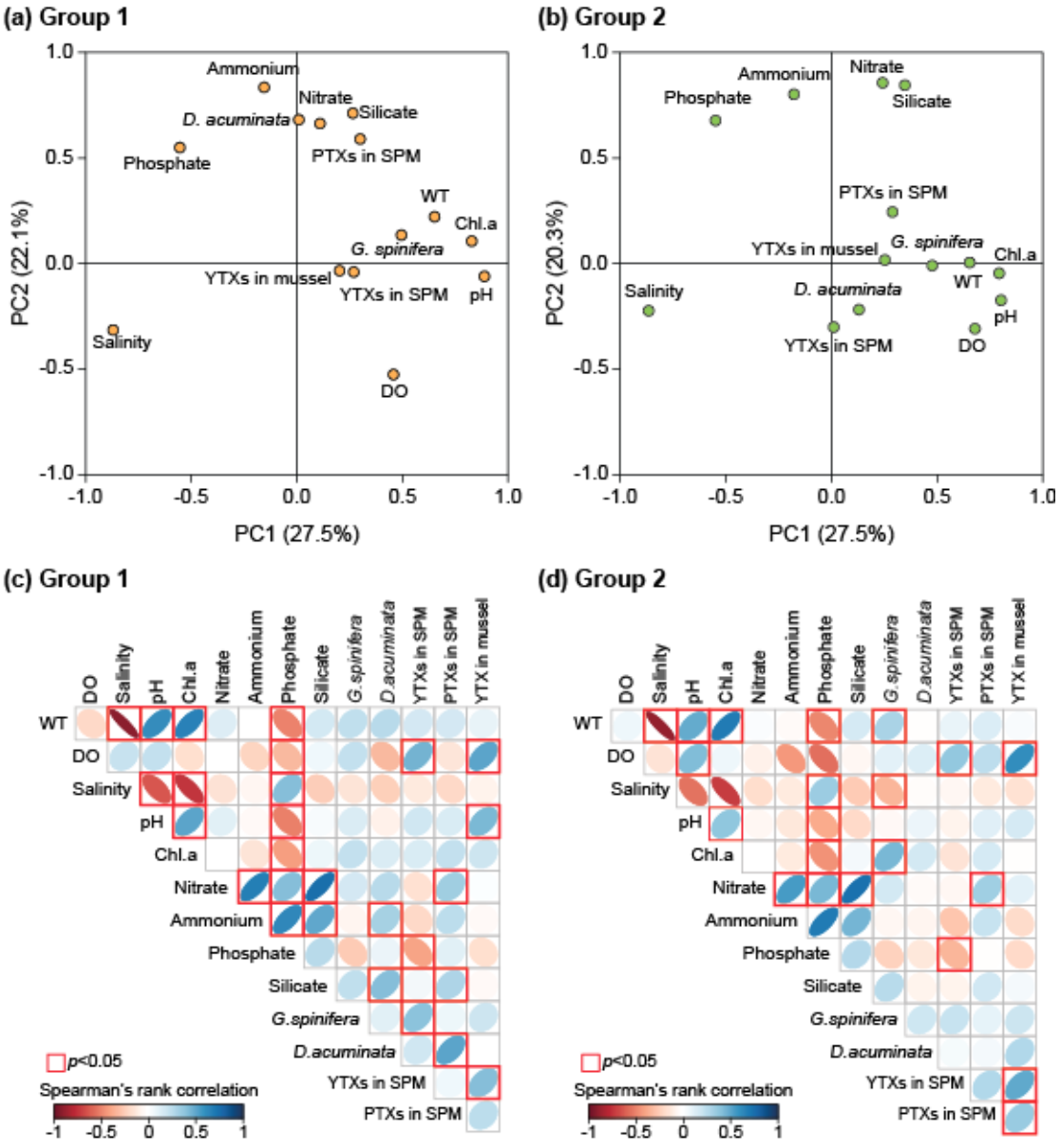

Fig. S3. Results of the principal component analysis (PCA) for **(a)** Group 1 and **(b)** Group 2. Spearman's rank correlation between environmental parameters, density of causative algae of YTXs and PTXs, and concentrations of YTXs and PTXs in phytoplankton and mussels in **(c)** Group 1 and **(d)** Group 2.